Tennessee State University
Digital Scholarship @ Tennessee State University

Mathematical Sciences Faculty Research | Department of Mathematical Sciences

10-12-2017

Computational modeling of high-entropy alloys: Structures, thermodynamics and elasticity

Michael C. Gao
AECOM

Pan Gao
Tennessee State University

Jeffrey A. Hawk
National Energy Technology Laboratory

Lizhi Ouyang
Tennessee State University

David E. Alman
National Energy Technology Laboratory

See next page for additional authors

Follow this and additional works at: https://digitalscholarship.tnstate.edu/mathematics

 Part of the Materials Science and Engineering Commons, and the Thermodynamics Commons

Recommended Citation

Gao, M.C., Gao, P., Hawk, J.A. et al. Computational modeling of high-entropy alloys: Structures, thermodynamics and elasticity. Journal of Materials Research 32, 3627–3641 (2017). https://doi.org/10.1557/jmr.2017.366

This Article is brought to you for free and open access by the Department of Mathematical Sciences at Digital Scholarship @ Tennessee State University. It has been accepted for inclusion in Mathematical Sciences Faculty Research by an authorized administrator of Digital Scholarship @ Tennessee State University. For more information, please contact XGE@Tnstate.edu.

Authors

Michael C. Gao, Pan Gao, Jeffrey A. Hawk, Lizhi Ouyang, David E. Alman, and Mike Widom

This article is available at Digital Scholarship @ Tennessee State University: https://digitalscholarship.tnstate.edu/mathematics/24

Computational Modeling of High-Entropy Alloys: Structures, Thermodynamics and Elasticity

Journal:	*Journal of Materials Research*
Manuscript ID	JMR-2017-0575.R2
Manuscript Type:	Review
Date Submitted by the Author:	n/a
Complete List of Authors:	Gao, Michael; National Energy Technology Laboratory Morgantown, Structural Materials Gao, Pan; Tennessee State University, Electrical and Computer Engineering Hawk, Jeffrey; National Energy Technology Laboratory, Structural Materials Ouyang, Lizhi; Tennessee State University , Department of Physics Alman, David; National Energy Technology Laboratory, Structural Materials Widom, Mike; Carnegie Mellon University, Physics
Key Words:	elastic properties, metal, phase equilibria

SCHOLARONE™
Manuscripts

For Review

Computational Modeling of High-Entropy Alloys: Structures, Thermodynamics and Elasticity

M. C. Gao[1,2*], P. Gao[3], J. A. Hawk[1], L. Z. Ouyang[3], D. E. Alman[1], and M. Widom[4]

[1]National Energy Technology Laboratory, Albany, OR 97321, USA.

[2]AECOM, P.O. Box 1959, Albany, OR 97321, USA.

[3]Tennessee State University, Nashville, TN 37209, USA.

[4]Carnegie Mellon University, Pittsburgh, PA 15213, USA.

*Correspondence: michael.gao@netl.doe.gov. Tel: +1-541-967-5869. Fax: +1-541-918-4493

For Peer Review

Abstract

This paper provides a short review on computational modeling on the formation, thermodynamics and elasticity of single-phase high-entropy alloys (HEAs). Hundreds of predicted single-phase HEAs were re-examined using various empirical thermo-physical parameters. Potential BCC HEAs (CrMoNbTaTiVW, CrMoNbReTaTiVW and CrFeMoNbReRuTaVW) were suggested based on CALPHAD modeling. The calculated vibrational entropies of mixing are positive for FCC CoCrFeNi, negative for BCC MoNbTaW, and near-zero for HCP CoOsReRu. The total entropies of mixing were observed to trend in descending order: CoCrFeNi > CoOsReRu > MoNbTaW. Calculated lattice parameters agree extremely well with averaged values estimated from the rule of mixtures (ROM) if the same crystal structure is used for the elements and the alloy. The deviation in the calculated elastic properties from ROM for select alloys is small, but is susceptible to the choice used for the structures of pure components.

Keywords: High-entropy alloys, Thermodynamics, Elasticity

1. Introduction

Since Yeh[1] and Cantor[2] independently reported their research on high-entropy alloys (HEAs) or equimolar multicomponent alloys in 2004, HEAs have attracted considerable interest from the scientific community, both in terms of developing a fundamental scientific understanding and potential technological applications.[3-5] However, to date a variety of important questions still remain: In particular, what factors govern the formation of single-phase solid solution HEAs? What are the total number of possible single-phase equimolar HEA alloys with the face-centered cubic (FCC), body-centered cubic (BCC), and hexagonal close-packed (HCP) structures, respectively? For each crystal structure type, what is the maximum number of components that a single-phase HEA can possibly dissolve at high temperatures? How can the thermodynamic properties of single-phase HEAs be accurately predicted, given the assumed disordered atomic structures? What other entropy sources are possible, given the fact that the definition of HEAs by Yeh is based on ideal configurational entropy? How can the elastic properties of single-phase HEAs be reliably calculated, and how do they compare with their pure components?

Empirical thermo-physical parameters,[6-18] CALPHAD modeling,[19-29] phase diagram inspection,[25, 30] *ab initio* molecular dynamics simulations (AIMD),[3, 25, 30, 31] hybrid Monte Carlo/molecular dynamic simulations (MC/MD),[32, 33] and first-principles density functional theory (DFT) calculations[3, 30, 33-37] have all been used to predict the formation of single-phase HEAs. Gao[30] first evaluated the strengths and weaknesses among these methodologies, and concluded that rationally combining these techniques will likely speed up identification of new single-phase HEA compositions. It was also suggested at the time that hundreds of quaternary and higher-order equimolar compositions in the Dy-Er-Gd-Ho-Lu-Sc-Sm-Tb-Tm-Y, Ba-Ca-Eu-

For Peer Review

Sr-Yb, and Mo-Nb-Re-Ta-Ti-V-W systems may exist.[30] This work continues that investigation of those new single-phase HEAs that were mainly predicted by Bei,[38] Troparevsky,[14] Senkov,[39] and Gao,[30] and also reports the possible existence of new potential septenary, octonary, and ennead BCC refractory HEAs. The thermodynamic mixing properties of FCC CoCrFeNi, BCC MoNbTaW, and HCP CoOsReRu are reviewed using CALPHAD, DFT and MC/MD methods. The calculated elastic properties of single-phase HEAs with the FCC and BCC structures based on DFT calculations are then compared with the average values estimated from the rule of mixtures (ROM).

2. Computational methodologies and details

2.1 DFT total energy calculations

The DFT calculations at zero temperature were performed using the VASP (Vienna Ab Initio Simulation Package),[40, 41] a plane-wave pseudo-potential software package. Projector augmented-wave (PAW) potentials[42] were used as supplied with VASP and the Perdew-Burke-Ernzerhof[43] gradient approximation for the exchange-correlation functional. The semi-core 3p/4p/5p electrons of Cr, Fe, Mn, Mo, Nb, Ni, Os, Re, Ru, Ta, and W are explicitly treated as valence. The special quasi-random structure (SQS) method[44, 45] was used to mimic the disordered atomic structures for equimolar HEAs as previously reported by Gao et al.[36] The cell size of the SQS models used in this work are: 64 atoms for quaternary HEAs, and 125, 125 and 160 atoms for quinary FCC, BCC, and HCP HEAs, respectively. For alloys that contain magnetic elements Co, Cr, Fe, Mn or Ni, collinear spin polarization (i.e., using ferromagnetic and anti-ferromagnetic spin configurations as initial input) were considered. The Brillouin-zone integrations were performed, using the Monkhorst–Pack k-point meshes.[46] The energy convergence with respect to k-points mesh is about 1-2 meV/atom. The plane-wave energy

For Peer Review

cutoff was held constant at 500 eV, 264 eV, and 322 eV for CoCrFeNi, MoNbTaW and CoOsReRu, respectively. All SQS models first underwent a volumetric relaxation only (i.e., fixing the lattice shape and ionic positions), followed by full relaxation under zero pressure until the energy convergence reached 1 meV/atom. For simplicity, the zero-point energy was neglected in this study. The enthalpy of formation was calculated by subtracting the composition–weighted total energies of the constituent elements in their ground state from the total energy of the alloy.

Lattice phonon calculations were done using the harmonic approximation. The vibrational entropy (S^{vib}) is calculated by:

$$S^{vib}(V,T) = 3k_B \int_0^{\infty} n^{vib}[(f_{BE}+1)\ln(f_{BE}+1) - f_{BE}\ln f_{BE}]d\varepsilon \quad (1)$$

where n^{vib} is the phonon density of states (DOS), and f_{BE} is the Bose-Einstein distribution function.

Electronic excitation across the Fermi level by migrating electrons from valance band to conduction band gives rise to electronic entropy (S^{elec}), which can be determined by:

$$S^{elec}(V,T) = -2k_B \int_{-\infty}^{\infty} n^{elec}\left[f_{FD}\ln f_{FD} + (1-f_{FD})\ln(1\text{-}f_{FD})\right]d\varepsilon \quad (2)$$

where n^{elec} is the electron density of states, and f_{FD} is Fermi-Dirac distribution function.

2.2 MC/MD hybrid simulations

The hybrid MC/MD method proposed by Widom et al.[32, 33] was used to calculate the configurational entropy. Supercells of 108, 128, and 96 atoms were used for FCC CoCrFeNi, BCC MoNbTaW, and HCP CoOsReRu, respectively. The simulations were done by alternating molecular dynamics at each temperature with Monte Carlo swaps, each performed from first

For Peer Review

principles using VASP. The canonical ensemble (NVT) (i.e., constant amount of substance, volume and temperature) was adopted for the FCC and BCC structures, and the isothermal-isobaric ensemble (NPT) (i.e., constant amount of substance, pressure and temperature) for the HCP structure. A minimum of 1000 MC steps with MD time steps of 10 or 20 fs were carried out for these three alloys, resulting in a total MD simulation time of greater than 10 ps. More details on the procedures used are provided elsewhere.[32, 33, 47, 48] The reduction in configurational entropy due to short-range chemical order can be calculated using the pairwise truncation of the Kikuchi cluster variation method (CVM):[49]

$$I = \sum_{i,j=1}^{N} y_{ij} ln\left(y_{ij}/c_i c_j\right) \quad (3)$$

where y_{ij} is the near neighbor correlations, and c_i and c_j are the mole fractions of elements *i* and *j*, respectively.

2.3 CALPHAD modeling

The CALPHAD calculations were carried out using TCNI8 thermodynamic database supplied by ThermoCalc™.[50] For equilibrium calculations, all phases are restored. To calculate the entropy of mixing of the FCC and BCC phases, the ordered $L1_2$ and B2 phases were rejected. The TCNI8 database covers the complete constituent binaries and limited ternaries.[50] Recent research[24-28] details the database development and applications of CALPHAD modeling for HEAs.

3. Structures and formation

3.1 Re-examining those predicted single-phase compositions[14, 30, 38, 39]

For Peer Review

The new single-phase HEAs that were collected in Ref.[30] were mainly predicted by Bei,[38] Troparevsky,[14] Senkov,[39] and Gao.[30] Note that Troparevsky[14] did not specify the crystal structures of their predicted single-phase HEAs. The thermodynamic properties of most of these compositions are unknown, and whether they would truly form a single-phase, solid solution in the as-cast condition awaits experimental verification. To begin, those reassessed empirical rules[48] will be applied to these alloys.

The equations to calculate the empirical parameters are provided in the section of Supplementary Materials. The widely used parameters include ideal configurational entropy (S_{ideal}^{conf}), enthalpy of mixing in the liquid phase (ΔH_{mix}^{liq}),[6] atomic size difference (δ),[6] the Ω –parameter,[7] average valence electron concentration ($\overline{VEC}$),[8] electronegativity difference ($\Delta\chi$),[9] the ϕ –parameter,[10] elastic residual strain root mean square ($\varepsilon_{R.M.S.}$, or $\sqrt{\langle\varepsilon^2\rangle}$),[11] the atomic size-related α_2 –parameter,[12] intrinsic elastic strain energy (E_2/E_0),[12] the Φ –parameter,[13] the η –parameter,[14, 48] and the κ_1^{cr} parameter.[15]

Very recently Gao et al.[48] assessed the most-up-to-date reported HEAs (single-phase, multiphase, and amorphous) and re-evaluated the effectiveness of those empirical rules. In general, the rules are useful since they are able to separate single-phase compositions from all amorphous compositions and many multiphase compositions. However, the threshold values are sensitive to the experimental data assessed, the atomic radii used, and whether or not two FCC or two BCC phases are counted as single-phase HEAs. They[48] found that the probably necessary requirements needed to form single-phase solid solutions are: -16.25 kJ/mol $\leq \Delta H_{mix}^{liq} \leq$ +5 kJ/mol, $\delta \leq 6\%$, $\Omega \geq 1$, $\eta \geq 0.19$, $\phi \geq 7.0$, $\varepsilon_{R.M.S.} \leq 0.061$, and $E_2/E_0 \leq 13.6 \times 10^{-4}$. However, these are not sufficient conditions, since many multiphase compositions also satisfy these criteria.

For Peer Review

The select empirical parameters of those predicted single-phase HEA compositions[30] are shown in Fig. 1, and all parameters evaluated in this work are summarized in Table S1 (Complementary Materials). Clearly the vast majority of the predicted compositions satisfy those reevaluated criteria by Gao et al.[48] The calculated $\Delta\chi$ values using the Pauling electronegativity are less than 0.36. Many compositions do not satisfy the $\Delta H_{IM}/\Delta H_{mix}^{liq} < \kappa_1^{cr}$[15] criterion.[15] Those compositions recommended by Troparevsky et al.[14] have $\overline{VEC}$ greater than 7.43, suggesting that most of them either prefer the FCC or HCP structure as the main phase in their microstructures (Fig. 1e). The average bulk and shear moduli were estimated using the rule of mixtures (ROM):

$$\overline{P} = \sum_i c_i P_i \quad (4)$$

where P_i refers to the properties of the i^{th} element (lattice parameter (a), elastic constants (C_{ij}), bulk modulus (B), and shear modulus (G)), and $\overline{P}$ refers to the corresponding average value for the alloy. The result is shown in Fig. 1(f). The HEAs that comprise of alkali earth and/or rare earth elements are very soft since their shear and bulk moduli are very small while other HEAs that contain high-melting transition metals have significantly higher shear and bulk moduli.

3.2 CALPHAD predictions: New septenary, octonary, and ennead BCC HEAs

Figure 2 shows the calculated equilibrium phase mole fraction as a function of temperature for septenary CrMoNbTaTiVW, octonary CrMoNbReTaTiVW, and ennead CrFeMoNbReRuTaVW, using the TCNI8 database.[51] The insets are the non-equilibrium solidification using the Scheil-Gulliver models,[52, 53] which assume equilibrium mixing in the liquid state and no diffusion in solid state. Both the equilibrium and Scheil simulations predict formation of single BCC solid solution in CrMoNbTaTiVW, CrMoNbReTaTiVW, while

For Peer Review

formation of C14 and HCP phases in very small fractions towards the end of the Scheil solidification are predicted for CrFeMoNbReRuTaVW.

It has been proposed[30] that a stable single-phase solid solution in as-cast state is promoted when there is a wide temperature range (T_{rd}) between the solidus temperature (T_{sol}) and decomposition temperature (T_{dec}):

$$T_{rd} = (T_{sol} - T_{dec})/T_{sol} \geq 0.3 \quad (5)$$

The calculated T_{rd} parameters from equilibrium thermodynamic calculation are 0.40, 0.43, and 0.29 for CrMoNbTaTiVW, CrMoNbReTaTiVW, and CrFeMoNbReRuTaVW, respectively. Both the Scheil simulations and the calculated T_{rd} values suggest that CrFeMoNbReRuTaVW may be on the verge of forming single BCC phase in the as-cast condition.

4. Entropy of mixing and entropy sources

4.1 Entropy of mixing calculated from CALPHAD

The compositional dependences of the entropy of mixing for the FCC phase in the Co-Cr-Fe-Mn-Ni system and the BCC phase in the Mo-Nb-Ta-V-W system at T=1273 K are illustrated in Fig. 3 using CALPHAD method. The ideal configurational entropies are also shown as reference in dashed lines. Due to presence of short range order, or segregation, and the contribution from lattice phonon vibration, or magnetic contribution, the total entropy of mixing (ΔS_{mix}^{φ}) for a HEAs may not always follow ideal mixing and can cause positive or negative deviation from $-R\sum_i c_i \ln c_i$ (i.e., excess entropy). The excess entropy (${}^{ex}S_{mix}^{\varphi}$) of a solution

For Peer Review

phase (φ) is calculated by subtracting the ideal configurational entropy from the total entropy of the alloy (ΔS_{mix}^{φ}):[28]

$$^{ex}S_{mix}^{\varphi} = \Delta S_{mix}^{\varphi} + R\sum_{i} c_i \ln c_i \quad (6)$$

The FCC phase in the Co-Cr-Fe-Mn-Ni system (Fig. 3a and 3b) exhibits positive deviation from the ideal mixing and thus positive excess entropy for equal and near-equimolar compositions. The maximum excess entropy becomes smaller with increasing number of components (Fig. 3b). The compositions with the highest ΔS_{mix}^{FCC} also do not necessarily occur at the equimolar compositions. In contrast, the BCC phase in the Mo-Nb-Ta-V-W system (Fig. 3c and 3d) shows a negative deviation from the ideal mixing and thus negative excess entropy at equal and near-equimolar compositions except the Mo-V binary which shows ideal mixing behavior (Fig. 3d). At equimolar compositions, the calculated entropy of mixing for both FCC and BCC phases increase with increasing number of components, suggesting the dominance of configurational entropy over other entropy sources at T=1273 K. However, the contrasting behavior in the excess entropy between FCC and BCC structures indicates the other entropy sources such as vibrational entropy of mixing may be also important, as revealed from DFT calculations (see the next subsection).

4.2 DFT calculations: Enthalpy of formation and entropy sources

In general SQS models tend to maximize random distributions of atoms in the lattice, but the permutation in the atomic position between elements may alter the local atomic environment and accordingly the fluctuation in the energy. The total number of atomic configurations for a HEA SQS model that result from atomic permutation scales up almost exponentially with increasing the number of equimolar components, and it is 24 for an equimolar quaternary HEA (

For Peer Review

$4!=24$) and 120 for an equimolar quinary HEA ($5!=120$). To examine the effect of element permutation on the enthalpy of formation (ΔH_{SS}), DFT calculations were carried out on all 24 configurations of FCC CoCrFeNi, BCC MoNbTaW, and HCP CoOsReRu, and the results are shown in Fig. 4a. The averaged ΔH_{SS} are 8.354 ± 0.266 kJ/mol, -7.407 ± 0.069 kJ/mol, and 2.724 ± 0.49 kJ/mol for CoCrFeNi, MoNbTaW, and CoOsReRu, respectively. Relatively speaking, CoOsReRu is a bit more sensitive to the atomic configuration than the other two structures, presumably due to the anisotropy of the HCP structure compared to the cubic structure. Other factors that may also contribute to the sensitivity with respect to the atomic configuration in SQS models are electronegativity, magnetism, and atomic size of the constituent elements. It can be assumed that this sensitivity may decrease with increasing SQS cell size which, however, may increase the computing time substantially.

The calculated ΔH_{SS} for widely studied single-phase HEAs are shown in Fig. 4b. Note that only one randomly chosen atomic configuration of the SQS model was used in the calculations (except CoCrFeNi, MoNbTaW, and CoOsReRu whose averaged ΔH_{SS} was used), so small fluctuation in ΔH_{SS} is expected upon atomic permutation tests. For FCC and HCP HEAs, the calculated ΔH_{SS} are positive, or close to zero. BCC AlNbTiV has the most negative ΔH_{SS} at -10.3 kJ/mol, followed by BCC MoNbTaW. Addition of HCP metals such as Hf, Ti and Zr to BCC refectory metals causes a near-zero, or even positive, ΔH_{SS}.

The electronic density of states (DOS) for FCC CoCrFeNi, BCC MoNbTaW, and HCP CoOsReRu is shown in Fig. 5. Integration of the difference between spin-up and spin-down electronic DOS gives rise to the magnetic moment, which is 0.62 ± 0.03 μ_B/atom for CoCrFeNi and 0.11 ± 0.02 μ_B/atom for CoOsReRu (here μ_B = Bohr magneton), averaged from total 24

For Peer Review

atomic configurations. A clear pseudo-gap exists only for MoNbTaW, and the Fermi level sits on the left edge to the gap. Existence of a deep pseudo-gap of an alloy usually suggests thermodynamic stability, and this is consistent with the negative ΔH_{SS} of -7.407 kJ/mol for BCC MoNbTaW. Conversely, the Fermi levels of CoCrFeNi and CoOsReRu sit on (relatively speaking) a plateau with low DOS.

The entropy sources of a solid solution phase may comprise contributions from lattice vibration (S^{vib}), configuration (S^{conf}), electronic excitation (S^{elec}), and magnetic spin fluctuations (S^{mag}):

$$S^{total} = S^{vib} + S^{conf} + S^{elec} + S^{mag} \quad (7)$$

Since the critical magnetic ordering temperatures for FCC CoCrFeNi and CoCrFeMnNi are well below room temperature,[54, 55] it is sensible to assume that their magnetic entropy term should be temperature independent and thus can be ignored at T ≥ 293 K for simplicity. The HCP CoOsReRu HEA was first suggested by Gao and Alman,[25] and there are no experiments yet reported.

Figure 6a presents the phonon DOS of FCC CoCrFeNi, BCC MoNbTaW, and HCP CoOsReRu. Excellent agreement in the phonon DOS for CoCrFeNi with the experiment[54] is evident. At low energies (less than 10 meV), the phonon DOS is comparable for CoCrFeNi and CoOsReRu, but both are smaller than MoNbTaW. In contrast, the calculated vibrational heat capacity (C_V, see Fig. 6b) is very similar for all three alloys although it is slightly larger for CoOsReRu and MoNbTaW than CoCrFeNi at T ≤ 400 K. At higher temperatures, vibrational C_V approaches the theoretical limit 3R.

For Peer Review

Alloy entropies of mixing (ΔS_{mix}) are calculated by subtracting the composition–weighted total entropies of the constituent elements from the entropy of the alloy for total entropy, vibrational entropy, and electronic entropy, respectively. DFT-calculated total vibrational and electronic entropies for FCC CoCrFeNi, BCC MoNbTaW, and HCP CoOsReRu were reported elsewhere.[36, 48] The vibrational entropies of pure elements of FCC Co, BCC Cr, antiferromagnetic FCC Fe, and FCC Ni were used. FCC Cr was not discarded because of presence of 64 imaginary vibrational modes (out of a total of 324 modes) and its elastic instability.

The calculated ΔS_{mix} from various entropy sources for these HEAs are shown in Fig. 6c. The calculated entropies of mixing for these three HEAs in descending order are: $S^{conf} >> \left|\Delta S_{mix}^{vib}\right| >> \left|\Delta S_{mix}^{elec}\right|$. At a temperature close to the solidus temperatures, the calculated S^{conf} are fairly close to their ideal value ($R \ln 4$), and start to decrease very gradually until the temperature reaches 1100 K. At lower temperatures, S^{conf} decreases rapidly, signaling the development of chemical short-range order in the alloys. Note that S^{conf} at room temperature is much lower for MoNbTaW than for the others due to the tendency in forming the ordered BCC (i.e., B2) as revealed by Widom et al.[32, 47] The vibrational entropies of mixing (ΔS^{vib}) approach constant values at temperatures above the Debye temperature (i.e., T ≥ ~400 K), namely, +2.8 J/K/mol, -3.6 J/K/mol and -0.4 J/K/mol for CoCrFeNi, MoNbTaW and CoOsReRu, respectively. This is because the heat capacities approach their classical limit at 3R. In contrast, the calculated ΔS_{mix}^{elec} values are close to zero. The sum of all entropy sources shows that the total entropy of mixing in descending order for these alloys is: CoCrFeNi > CoOsReRu > MoNbTaW (Fig. 6d).

5. Elastic properties

For Peer Review

Single-crystal elastic constants (C_{ij}) are derived by performing six finite distortions of the lattice as implemented in VASP[56, 57] through the basic elastic stress-strain relationship:

$$\sigma_i = \sum_{j=1}^{6} C_{ij}\varepsilon_j \tag{8}$$

where σ_i, ε_j and C_{ij}, are the elastic stress, strain, and tensor in the Voigt notation, respectively. Since the local chemical environment in a SQS lattice may not be perfectly random or isotropic for HEAs, an averaging scheme proposed by Gao et al.[57] to obtain single–crystal C_{11}, C_{12} and C_{44} for cubic structures was adopted in this work:

$$\begin{aligned} C_{11} &= \frac{C_{11} + C_{22} + C_{33}}{3} \\ C_{12} &= \frac{C_{12} + C_{23} + C_{13}}{3} \\ C_{44} &= \frac{C_{44} + C_{55} + C_{66}}{3} \end{aligned} \tag{9}$$

The polycrystalline bulk modulus is determined by:

$$B = \frac{1}{3}(C_{11} + 2C_{22}) \tag{10}$$

The polycrystalline shear modulus (G) is estimated as the simple average of G_V and G_R, which are given by:

$$\begin{aligned} G_V &= \frac{\left(C_{11} - C_{12} + 3C_{44}\right)}{5} \\ G_R &= \frac{5\left(C_{11} - C_{12}\right)C_{44}}{4C_{44} + 3\left(C_{11} - C_{12}\right)} \end{aligned} \tag{11}$$

Poisson's ratio (ν) of the alloy can be derived from the bulk modulus (B) and the shear modulus (G) of the alloy:

$$\nu = \frac{3B-2G}{2(3B+G)} \tag{12}$$

For Peer Review

The average Poisson's ratio ($\overline{\nu}$) of the alloy was estimated by:

$$\overline{\nu} = \frac{3\overline{B}-2\overline{G}}{2(3\overline{B}+\overline{G})} \quad (13)$$

where $\overline{B}$ and $\overline{G}$ are the average bulk modulus and shear modulus of the alloy estimated using the ROM.

The necessary and sufficient conditions for cubic crystals to be mechanically stable are proposed by Born and Huang:[58]

$$C_{11} - C_{12} > 0;\ C_{11} + 2C_{12} > 0;\ C_{44} > 0 \quad (14)$$

Consequently, the Poisson's ratio of a mechanical stable crystals should be: $-1 < \nu < 0.5$. However, Feng and Widom[59] showed that elements Hf, Ti, and Zr in the BCC structure are mechanically unstable, since their DFT calculations predict $C_{12} > C_{11}$. For consistency in the comparison, the lattice parameters and elastic properties of BCC Hf, Ti and Zr calculated by Feng and Widom,[59] Tian et al.,[60] and Ge et al.[61] were used to calculate the average properties of BCC HEAs (see Table S2 in Supplementary Materials). Similarly, the present DFT work predicts the elastic constants of FCC Cr to be: C_{11}=26 GPa, C_{12}=348 GPa, C_{44}=-87 GPa, resulting in unphysical values of G=-112 GPa and ν=0.78. In contrast, the calculated elastic properties of BCC Cr in antiferromagnetic state are: C_{11}=434 GPa, C_{12}=59 GPa, C_{44}=96 GPa, B=184 GPa, G=126 GPa, ν=0.22, and they satisfy the stability criteria set by Eq. (14). Therefore, the mechanically stable BCC Cr is used instead to calculate the average properties of FCC CoCrFeNi and FCC CoCrFeMnNi in the present work (see Table S3 in Supplementary Materials).

The lattice parameters and elastic properties of select equimolar HEAs that were computationally studied by Gao et al.,[36] Feng and Widom,[59] Tian et al.,[60] and Ge et al.,[61] were assessed in this work. Four ternary BCC, eight quaternary BCC, two quinary BCC, one

For Peer Review

quaternary FCC, and one quinary FCC equimolar alloys were studied. The elastic properties of single-phase HEAs were previously reviewed by Gao et al.[36] and Tian et al. [35, 62] The data are provided in Table S4 (Supplementary Materials), and the comparison in the lattice parameters and elastic properties between DFT calculations and the ROM are shown in Fig. 7. For BCC HEAs, DFT calculations slightly underestimated the lattice parameter compared with the averaged values (Fig. 7a). For FCC CoCrFeNi and CoCrFeMnNi, DFT calculations overestimated the lattice parameters compared with the averaged values presumably because the lattice parameter of BCC Cr with two atoms in the unit cell, which is significantly smaller than that of FCC Cr (see Table S3), was used for the ROM. Excellent agreement in C_{11} between calculations and averages is observed except the FCC HEAs (Fig. 7b) probably because the property of BCC Cr was used. The C_{12} values scatter much more widely than C_{11} or C_{44} (Fig. 7b-d). The distribution of B, G and ν is close to the equality lines with minor scatter (Fig. 7e-g).

6. Discussion

Predicting the formation of single-phase HEA compositions has been an intense research topic,[3, 6-36, 63] and yet the total number of single-phase HEAs confirmed by experiments is still very limited.[30, 48] Single-phase HEAs with the total number of principal elements greater than five are very scarce, including senary compositions (HfNbTaTiVZr,[21] MoNbTaTiVW,[29] CrMoNbTaVW,[29] and MoNbReTaVW[38]) and septenary compositions (MoNbReTaTiVW,[38] CrMoNbReTaVW,[64] and CuIrNiPdPtRh[65]). Strictly speaking, formation of single-phase HEAs is the direct consequence of multiphase competition as a function of temperature and composition towards minimizing the total Gibbs free energy of the system, and thus the CALPHAD method is the ideal tool for tackling phase stability in a multicomponent systems such as HEAs. However, most commercial databases are intended for compositions that are enriched in the principal

For Peer Review

element and thus simple extrapolation to the compositional center of a phase diagram may produce inaccurate or even wrong predictions. Other databases that are dedicated to HEAs may not cover all constituent binaries and ternaries in their entire composition and temperature ranges. Other roadblocks to developing a reliable database include lack of sufficient experimental data and/or the lack of physically-meaningful descriptions for those hypothetical phases such as endmembers and antiphases.[28, 48]

Gao et al.[48] also analyzed the weakness of those empirical parameters, which included the underlying hypotheses, oversimplified treatment of the entropy of mixing for the solution phase, and the oversimplified treatment of enthalpy of intermetallic phases. However, if the CALPHAD databases are not available or do not cover all the binaries and ternaries, phase diagram inspection or employing available empirical thermo-physical parameters become especially important in quick selection of promising elements that are most likely to promote the formation of solid solution phases as opposed to intermetallic phases. Gao[30] first summarized that, those experimentally confirmed single-phase HEAs exhibit either isomorphous solid solution (e.g., the Nb-Mo-Ta-W and Hf-Nb-Ta-Ti-Zr systems), or quite large terminal solubilities (e.g., Co-Fe-Mn-Ni system) in their constituent binaries and ternaries. Gao[30] further highlighted three types of solid solutions in a phase diagram that are important for HEA formation: (1) Isomorphous solid solution (e.g., the FCC phase in the Co-Ni binary and the HCP phase in the Re-Ru binary), (2) extended terminal solid solubility (e.g., the BCC and HCP phases in the Cr-Ru binary), and (3) intermediate solid solution (e.g., the HCP phase in the Cr-Rh binary).

Good agreement in predicting the entropy of mixing between DFT calculations and CALPHAD was obtained in the present study. More importantly, DFT calculations illuminated the entropy sources of HEAs and revealed that the positive vibrational entropy of mixing in FCC

For Peer Review

CoCrFeNi mainly contributes to its positive excess entropy. Alternatively, the negative vibrational entropy of mixing in BCC MoNbTaW mainly contributes to its negative excess entropy. The sign of the vibrational entropy of mixing (Fig. 5c) for FCC CoCrFeNi and BCC MoNbTaW seems to coincide with the sign of their enthalpies of formation (Fig. 4b). The presence of strong short-range order in BCC MoNbTaW[32, 33] causes a larger negative enthalpy of formation, decreases the average atomic volume, and hence, promotes an increase in the phonon vibrational frequency. Conversely, a larger positive enthalpy of formation in FCC CoCrFeNi may enlarger the overall bond length, and hence, increase the average atomic volume while potentially decreasing phonon vibrational frequency. The enthalpy of formation of HCP CoOsReRu is close to zero, and this suggests negligible bond formation in the alloy which may have little impact on the phonon vibrational frequency. Indeed, the calculated vibrational entropy of mixing is zero for HCP CoOsReRu.

At T > 400 K, the calculated vibrational entropy of mixing is +2.8, -3.6 and -0.3 J/K/mol for FCC CoCrFeNi, BCC MoNbTaW and HCP CoOsReRu, respectively. Calculated entropies of mixing for these three HEAs in descending order are: $S^{conf} >> \left|\Delta S_{mix}^{vib}\right| >> \left|\Delta S_{mix}^{elec}\right|$. Although the calculated configurational entropies approach the theoretical limit at high temperatures close to their melting points, developing short-range order can cause a sharp decrease in the configurational entropy at low temperatures. As a result, the total entropy of mixing of an HEA depends on the configurational entropy as well as vibrational entropy of mixing, and is more sensitive to temperature at intermediate and low temperatures. The total entropies of mixing (i.e., $\Delta S_{mix}^{vib} + \Delta S_{mix}^{elec} + S^{conf}$) were observed to trend in the following manner: CoCrFeNi > CoOsReRu > MoNbTaW at T ≥ 300 K.

For Peer Review

The solid solution stabilization by phonon vibration was also reported by Fultz et al.[66] who measured ΔS_{mix}^{vib} to be +1.17, +1.67 and +1.78 J/K/mol for disordered BCC solid solution alloys $Fe_{70}Cr_{30}$, $Fe_{53}Cr_{47}$ and $Fe_{30}Cr_{70}$, respectively. However, it is generally not obvious whether a chemical disordering causes positive or negative vibrational entropy of mixing, or whether a disordered alloy will exhibit greater vibrational entropy than its ordered form. The vibrational entropy of mixing of an alloy may depend on the crystal structure, bonding and enthalpy of the alloy, as well as the molar volumes and structures of the constituent elements.[67] For example, Munoz et al.[68] found that the chemical ordering in the B2 structure increases the vibrational entropy by 1.83 J/K/mol, compared to the disordered B2 FeV alloy.

Elastic properties (such as elastic constants and bulk/shear moduli) of a solid solution primarily depend on the interatomic interactions among constituent elements. Intuitively speaking, electron hybridization may result in strong attractive interaction, and accordingly, shortened bond length and negative enthalpy of formation (ΔH_{ss}). Conversely, repulsive interaction may result in positive enthalpy of formation. However, for BCC MoNbTaW that has an ΔH_{ss} of -7.4 kJ/mol, its lattice parameter, elastic constants, and average bulk and shear moduli agree well with the averages estimated from ROM. To further examine the distribution of the calculated properties (a, C_{11}, C_{12}, C_{44}, B, G and ν) with respect to the averaged values from ROM, the change in the properties in percentage is shown in Fig. 8. The maximum ranges in $\Delta P / P_{avg}$ are: 0.6% for a except 6.1% for CoCrFeNi and 4.9% for CoCrFeMnNi, 32% for C_{11}, 23% for C_{12}, 86% for C_{44} , 20% for B, 28% for G except extreme cases (143% for HfNbTaZr, and 53% for NbTiVZr), and 16% for ν. In order to make a meaningful comparison with respect to the averaged values, the properties of the pure elements in the same crystal structure as the alloy should be used. However, certain elements are mechanically unstable in certain structures,

For Peer Review

such as FCC Cr and BCC Hf/Ti/Zr, and thus, it is controversial whether it is appropriate to use their properties, although seemingly unphysical, to calculate averaged properties via the ROM.

6. Conclusions

This work evaluated the empirical thermo-physical parameters for hundreds of single-phase HEAs that were predicted using empirical parameters, CALPHAD and phase diagram inspections. New septenary, octonary, and ennead BCC refractory HEAs were suggested. Entropy of mixing for example HEAs were modeled using CALPHAD, DFT, and MC/MD methods. The elastic properties of HEAs were evaluated. The following conclusions were reached:

1. The vast majority of those predicted single-phase HEAs[30] satisfy the reevaluated empirical rules by Gao et al.[48] except the $\Delta H_{IM}/\Delta H_{mix}^{liq} < \kappa_1^{cr}$ criterion.[15] However, whether they form single-phase solid solution awaits future experiment examination.
2. Calculated $\overline{VEC}$ values hypothesize that the majority of the alloys suggested by Troparevsky et al.[14] may have the FCC or HCP structures as the main phase in the microstructure.
3. Equilibrium calculations, Sheil simulations and T_{rd} parameters using TCNI8 database suggest that septenary CrMoNbTaTiVW and octonary CrMoNbReTaTiVW likely form BCC HEAs while ennead CrFeMoNbReRuTaVW may be on the border between single-phase and multiphase.
4. TCNI8 database predicts a total entropy of mixing of 13.7 J/K/mol for FCC CoCrFeNi and 10.4 J/K/mol for BCC MoNbTaW at T=1273 K, which corresponds to excess entropy of +2.2 and -1.2 J/K/mol, respectively.

For Peer Review

5. DFT-calculated averaged enthalpy of formation for FCC CoCrFeNi, BCC MoNbTaW, and HCP CoOsReRu, 8.354±0.266 kJ/mol, -7.407±0.069 kJ/mol, and 2.724±0.49 kJ/mol, respectively, resulting from 24 atomic configurations due to permutation between elements.
6. DFT calculated enthalpy of formation of twenty-one single-phase solid solution HEAs are: -10.3 kJ/mol < ΔH_{ss} < +8.4 kJ/mol.
7. Calculated configurational entropies (S^{conf}) for CoCrFeNi, MoNbTaW and CoOsReRu alloys were fairly equivalent to their ideal value (R ln 4) at temperatures close to their solidus temperatures. However, S^{conf} at room temperature is much lower for MoNbTaW than the others due to the tendency in forming the ordered BCC (i.e., B2) as revealed by Widom et al.[32, 47]
8. DFT-calculated phonon DOS for FCC CoCrFeNi is in excellent agreement with the experiment by Lucas et al.[54] At T > 400 K, the calculated vibrational entropy of mixing is +2.8, -3.6 and -0.3 J/K/mol for FCC CoCrFeNi, BCC MoNbTaW and HCP CoOsReRu, respectively. Calculated entropies of mixing for these three HEAs in descending order are: $S^{conf} >> \left|\Delta S_{mix}^{vib}\right| >> \left|\Delta S_{mix}^{elec}\right|$.
9. DFT calculations illuminate the entropy sources of HEAs and reveal that the positive vibrational entropy of mixing in FCC CoCrFeNi mainly contributes to its positive excess entropy while the negative vibrational entropy of mixing in BCC MoNbTaW mainly contributes to its negative excess entropy.
10. The total entropies of mixing (i.e., $\Delta S_{mix}^{vib} + \Delta S_{mix}^{elec} + S^{conf}$) were observed to trend in the following manner: CoCrFeNi > CoOsReRu > MoNbTaW.
11. The maximum ranges in the properties with respect the averaged values estimated from the ROM (i.e., $\Delta P / P_{avg}$) are: 0.6% for lattice parameter a except 6.1% for CoCrFeNi and 4.9%

For Peer Review

for CoCrFeMnNi, 32% for C_{11}, 23% for C_{12}, 86% for C_{44}, 20% for bulk modulus B, 28% for shear modulus G except extreme cases (143% for HfNbTaZr, and 53% for NbTiVZr), 16% for Poisson's ratio ν.

12. The uncertainties in the elastic properties for certain elements that are mechanically unstable in certain crystal structures (e.g., FCC Cr, BCC Hf/Ti/Zr) may lead to biased results when estimating the average properties using the ROM (e.g., using FCC Cr vs BCC Cr, using BCC Hf/Ti/Zr vs HCP Hf/Ti/Zr).

Acknowledgements

This work was carried out in support of the Cross-Cutting Technologies Program at the National Energy Technology Laboratory (NETL), managed by Robert Romanosky (Technology Manager). The Research was executed through NETL's Research and Innovation Center's Innovative Process Technologies (IPT) Field Work Proposal. Research performed by AECOM Staff was conducted under the RES contract DE-FE-0004000. L.Z. Ouyang acknowledges support by DE-FE-0011549 and DE-NA0002630. Work at Carnegie Mellon was supported under grant DE-SC0014506.

***Disclaimer**: The computational modeling work presented in the paper is project was funded by the Department of Energy, National Energy Technology Laboratory, an agency of the United States Government, through a support contract with AECOM. Neither the United States Government nor any agency thereof, nor any of their employees, nor AECOM, nor any of their employees, makes any warranty, expressed or implied, or assumes any legal liability or responsibility for the accuracy, completeness, or usefulness of any information, apparatus, product, or process disclosed, or represents that its use would not infringe privately owned rights. Reference herein to any specific commercial product, process, or service by trade name,*

For Peer Review

trademark, manufacturer, or otherwise, does not necessarily constitute or imply its endorsement, recommendation, or favoring by the United States Government or any agency thereof. The views and opinions of authors expressed herein do not necessarily state or reflect those of the United States Government or any agency thereof.

The empirical thermo-physical rules, predicted single-phase compositions and their geometric and thermo-physical parameters, and DFT-calculated lattice parameters and elastic properties for pure elements and select alloys are provided in the Supplementary Materials.

References

1. J.W. Yeh, S.K. Chen, S.J. Lin, J.Y. Gan, T.S. Chin, T.T. Shun, C.H. Tsau and S.Y. Chang: Nanostructured High-Entropy Alloys with Multiple Principal Elements: Novel Alloy Design Concepts and Outcomes *Adv. Eng. Mater.* **6**(5), 299 (2004).

2. B. Cantor, I.T.H. Chang, P. Knight and A.J.B. Vincent: Microstructural development in equiatomic multicomponent alloys *Mater. Sci. Eng. A.* **375–377**, 213 (2004).

3. Y. Zhang, T.T. Zuo, Z. Tang, M.C. Gao, K.A. Dahmen, P.K. Liaw and Z.P. Lu: Microstructures and Properties of High-entropy Alloys *Prog. Mater. Sci.* **61**, 1 (2014).

4. M.C. Gao, J.W. Yeh, P.K. Liaw and Y. Zhang: High-Entropy Alloys: Fundamentals and Applications, 1st ed. (Springer International Publishing, City, 2016), p.^pp. 516.

5. D.B. Miracle and O.N. Senkov: A critical review of high entropy alloys and related concepts *Acta Mater.* **122**, 448 (2017).

6. Y. Zhang, Y.J. Zhou, J.P. Lin, G.L. Chen and P.K. Liaw: Solid-Solution Phase Formation Rules for Multi-component Alloys *Adv. Eng. Mater.* **10**(6), 534 (2008).

7. Y. Zhang, Z.P. Lu, S.G. Ma, P.K. Liaw, Z. Tang, Y.Q. Cheng and M.C. Gao: Guidelines in predicting phase formation of high-entropy alloys *MRS Comm.* **4**(02), 57 (2014).

8. S. Guo, C. Ng, J. Lu and C.T. Liu: Effect of valence electron concentration on stability of fcc or bcc phase in high entropy alloys *J. Appl. Phys.* **109**(10), 103505 (2011).

9. S. Fang, X. Xiao, L. Xia, W. Li and Y. Dong: Relationship between the widths of supercooled liquid regions and bond parameters of Mg-based bulk metallic glasses *J. Non-Cryst. Solids.* **321**, 120 (2003).

For Peer Review

10. Y.F. Ye, Q. Wang, J. Lu, C.T. Liu and Y. Yang: Design of high entropy alloys: A single-parameter thermodynamic rule *Scripta Mater.* **104**, 53 (2015).

11. Y.F. Ye, C.T. Liu and Y. Yang: A geometric model for intrinsic residual strain and phase stability in high entropy alloys *Acta Mater.* **94**, 152 (2015).

12. Z.J. Wang, W.F. Qiu, Y. Yang and C.T. Liu: Atomic-size and lattice-distortion effects in newly developed high-entropy alloys with multiple principal elements *Intermetallics.* **64**, 63 (2015).

13. D.J.M. King, S.C. Middleburgh, A.G. McGregor and M.B. Cortie: Predicting the formation and stability of single phase high-entropy alloys *Acta Mater.* **104**, 172 (2016).

14. M.C. Troparevsky, J.R. Morris, P.R.C. Kent, A.R. Lupini and G.M. Stocks: Criteria for Predicting the Formation of Single-Phase High-Entropy Alloys *Phys. Rev. X.* **5**(1), 011041 (2015).

15. O.N. Senkov and D.B. Miracle: A new thermodynamic parameter to predict formation of solid solution or intermetallic phases in high entropy alloys *J. Alloys Compd.* **658**, 603 (2016).

16. M.G. Poletti and L. Battezzati: Electronic and thermodynamic criteria for the occurrence of high entropy alloys in metallic systems *Acta Mater.* **75**, 297 (2014).

17. I. Toda-Caraballo and P.E.J. Rivera-Diaz-del-Castillo: A criterion for the formation of high entropy alloys based on lattice distortion *Intermetallics.* **71**, 76 (2016).

18. S. Guo: Phase selection rules for cast high entropy alloys: an overview *Mater. Sci. Tech.* **31**(10), 1223 (2015).

19. M.C. Gao, C.S. Carney, Ö.N. Doğan, P.D. Jablonksi, J.A. Hawk and D.E. Alman: Design of Refractory High-Entropy Alloys *JOM.* **67**(11), 2653 (2015).

20. B. Zhang, M.C. Gao, Y. Zhang and S.M. Guo: Senary Refractory High-Entropy Alloy Cr_xMoNbTaVW *CALPHAD.* **51**, 193 (2015).

21. M.C. Gao, B. Zhang, S. Yang and S.M. Guo: Senary Refractory High-Entropy Alloy HfNbTaTiVZr *Metall. Mater. Trans. A.* **47A**, 3333 (2016).

22. H.W. Yao, J.W. Qiao, M.C. Gao, J.A. Hawk, S.G. Ma, H.F. Zhou and Y. Zhang: NbTaV-(Ti, W) Refractory High Entropy Alloys *Mater. Sci. Eng. A.* **674**, 203 (2016).

23. H.W. Yao, J.W. Qiao, M.C. Gao, J.A. Hawk, S.G. Ma and H.F. Zhou: MoNbTaV Medium-Entropy Alloy *Entropy.* **18**, 189 (2016).

24. C. Zhang, F. Zhang, S.L. Chen and W.S. Cao: Computational Thermodynamics Aided High-Entropy Alloy Design *JOM.* **64**(7), 839 (2012).

For Peer Review

25. M.C. Gao and D.E. Alman: Searching for Next Single-Phase High-Entropy Alloy Compositions *Entropy.* **15**, 4504 (2013).

26. F. Zhang, C. Zhang, S.L. Chen, J. Zhu, W.S. Cao and U.R. Kattner: An understanding of high entropy alloys from phase diagram calculations *CALPHAD.* **45**, 1 (2014).

27. O.N. Senkov, J.D. Miller, D.B. Miracles and C. Woodward: Accelerated exploration of multi-principal element alloys for structural applications *CALPHAD.* **50**, 32 (2015).

28. C. Zhang and M.C. Gao: CALPHAD Modeling of High-Entropy Alloys, in High-Entropy Alloys: Fundamentals and Applications, edited by M. C. Gao, J. W. Yeh, P. K. Liaw and Y. Zhang (Springer International Publishing, City, 2016), pp. 399.

29. B. Zhang, M.C. Gao, Y. Zhang, S. Yang and S.M. Guo: Senary Refractory High-Entropy Alloy MoNbTaTiVW *Mater. Sci. Tech.* **31**, 1207 (2015).

30. M.C. Gao: Design of High-Entropy Alloys, in High-Entropy Alloys: Fundamentals and Applications, edited by M. C. Gao, J. W. Yeh, P. K. Liaw and Y. Zhang (Springer International Publishing, City, 2016), pp. 369.

31. M.C. Gao, B. Zhang, S.M. Guo, J.W. Qiao and J.A. Hawk: High-Entropy Alloys in Hexagonal Close Packed Structure *Metall. Mater. Trans. A.* **47A**, 3322 (2016).

32. M. Widom, W.P. Huhn, S. Maiti and W. Steurer: Hybrid Monte Carlo/Molecular Dynamics Simulation of a Refractory Metal High Entropy Alloy *Metall. Mater. Trans. A.* **45A**(1), 196 (2014).

33. M. Widom: Prediction of structure and phase transformations, in High-Entropy Alloys: Fundamentals and Applications, edited by M. C. Gao, J. W. Yeh, P. K. Liaw and Y. Zhang (Springer International Publishing, City, 2016), pp. 267.

34. F.Y. Tian, L. Delczeg, N.X. Chen, L.K. Varga, J. Shen and L. Vitos: Structural stability of NiCoFeCrAlx high-entropy alloy from ab initio theory *Phys. Rev. B.* **88**(8), 085128 (2013).

35. F.Y. Tian, Y. Wang, D.L. Irving and L. Vitos: Applications of Coherent Potential Approximation to HEAs, in High-Entropy Alloys: Fundamentals and Applications, edited by M. C. Gao, J. W. Yeh, P. K. Liaw and Y. Zhang (Springer International Publishing, City, 2016), pp. 299.

36. M.C. Gao, C. Niu, C. Jiang and D.L. Irving: Applications of Special Quasi-Random Structures to High-Entropy Alloys, in High-Entropy Alloys: Fundamentals and Applications, edited by M. C. Gao, J. W. Yeh, P. K. Liaw and Y. Zhang (Springer International Publishing, City, 2016), pp. 333.

37. D. Ma, B. Grabowski, F. Kormann, J. Neugebauer and D. Raabe: Ab initio thermodynamics of the CoCrFeMnNi high entropy alloy: Importance of entropy contributions beyond the configurational one. *Acta Mater.* **100**, 90 (2015).

For Peer Review

38. H. Bei: Multi-Component Solid Solution Alloys Having High Mixing Entropy, edited by USPC (UT-BATTELLE, LLC, Oak Ridge, TN, City, 2013), p. US20130108502 A1.

39. O.N. Senkov, J.D. Miller, D.B. Miracle and C. Woodward: Accelerated exploration of multi-principal element alloys with solid solution phases *Nature Comm.* **6**(1-10), 6529 (2015).

40. G. Kresse and J. Hafner: Ab initio molecular dynamics for liquid metals *Phys. Rev. B.* **47**, 558 (1993).

41. G. Kresse and J. Furthmüller: Efficient iterative schemes for ab initio total-energy calculations using a plane-wave basis set *Phys. Rev. B.* **54**, 11169 (1996).

42. P.E. Blochl: Projector augmented-wave method *Phys. Rev. B.* **50**(24), 17953 (1994).

43. J.P. Perdew, K. Burke and M. Ernzerhof: Generalized Gradient Approximation Made Simple *Phys. Rev. Lett.* **77**, 3865 (1996).

44. S.H. Wei, L.G. Ferreira, J.E. Bernard and A. Zunger: Electronic properties of random alloys: special quasirandom structures *Phys. Rev. B.* **42**(15), 9622 (1990).

45. A. Zunger, S.H. Wei, L.G. Ferreira and J.E. Bernard: Special quasirandom structures *Phys. Rev. Lett.* **65**(3), (1990).

46. H.J. Monkhorst and J.D. Pack: Special points for brillouin-zone integrations *Phys. Rev. B.* **13**(12), 5188 (1976).

47. W.P. Huhn and M. Widom: Prediction of A2 to B2 Phase Transition in the High-Entropy Alloy Mo-Nb-Ta-W *JOM.* **65**(12), 1772 (2013).

48. M.C. Gao, C. Zhang, P. Gao, F. Zhang, L.Z. Ouyang, M. Widom and J.A. Hawk: Thermodynamics of Concentrated Solid Solution Alloys *Curr. Opin. Solid State Mater. Sci.* **submitted**, (2017).

49. H. Ackermann, G. Inden and R. Kikuchi: Tetrahedron approximation of the cluster variation method for bcc alloys *Acta Metall.* **37**(1), 1 (1989).

50. B. Sundman, B. Jansson and J.O. Andersson: The Thermo-Calc databank system *CALPHAD.* **9**, 153 (1985).

51. Online source: ThermoCalc Software. Available at www.thermocalc.com.

52. G.H. Gulliver: The quantitative effect of rapid cooling upon the constitution of binary alloys *J. Inst. Metals.* **9**, 120 (1913).

53. E. Scheil: Comments on the layer crystal formation *Z. Metallkd.* **34**, 70 (1942).

54. M.S. Lucas, L. Mauger, J.A. Munoz, Y. Xiao, A.O. Sheets, S.L. Semiatin, J. Horwath and Z. Turgut: Magnetic and vibrational properties of high-entropy alloys *J. Appl. Phys.* **109**(7), 07E307 (2011).

For Peer Review

55. M.S. Lucas, D. Belyea, C. Bauer, N. Bryant, E. Michel, Z. Turgut, S.O. Leontsev, J. Horwath, S.L. Semiatin, M.E. McHenry and C.W. Miller: Thermomagnetic analysis of $FeCoCr_xNi$ alloys: Magnetic entropy of high-entropy alloys *J. Appl. Phys.* **113**(17), 17A923 (2013).

56. Y. Le Page and P. Saxe: Symmetry-general least-squares extraction of elastic data for strained materials from ab initio calculations of stress *Phy. Rev. B.* **65**, 104104 (2002).

57. M.C. Gao, Y. Suzuki, H. Schweiger, Ö.N. Doğan, J. Hawk and M. Widom: Phase Stability and Elastic Properties of Cr-V Alloys *J. Phys. Cond. Matter.* **25**, 075402 (2013).

58. M. Born and K. Huang: Dynamical Theory of Crystal Lattices, 1st ed. (Clarendon Press, City, 1954).

59. B. Feng and M. Widom: Elastic stability and lattice distortion of refractory high entropy alloys *Mater. Chem. Phys.* **in press**, (2017).

60. L.Y. Tian, G. Wang, J.S. Harris, D.L. Irving, J. Zhao and L. Vitos: Alloying effect on the elastic properties of refractory high-entropy alloys *Mater. Des.* **114**, 243 (2017).

61. H.J. Ge, F.Y. Tian and Y. Wang: Elastic and thermal properties of refractory high-entropy alloys from first-principles calculations *Computational Materials Science.* **128**, 185 (2017).

62. F.Y. Tian, L.K. Varga, J. Shen and L. Vitos: Calculating elastic constants in high-entropy alloys using the coherent potential approximation: Current issues and errors *Comp. Mater. Sci.* **111**, 350 (2016).

63. Z. Wang, S. Guo and C.T. Liu: Phase Selection in High-Entropy Alloys: From Nonequilibrium to Equilibrium *Jom.* **66**(10), 1966 (2014).

64. B.L. Zhang, Y. Mu, M.C. Gao, W.J. Meng and S.M. Guo: On single-phase status and segregation of an as-solidified septenary refractory high entropy alloy *Mrs Communications.* **7**(1), 78 (2017).

65. S.W. Sohn, Y.H. Liu, J.B. Liu, P. Gong, S. Prades-Rodel, A. Blatter, B.E. Scanley, C.C. Broadbridge and J. Schroers: Noble metal high entropy alloys *Scripta Materialia.* **126**, 29 (2017).

66. B. Fultz, L. Anthony, J.L. Robertson, R.M. Nicklow, S. Spooner and M. Mostoller: Phonon modes and vibrational entropy of mixing in Fe-Cr *Physical Review B.* **52**(5), 3280 (1995).

67. B. Fultz: Vibrational thermodynamics of materials *Progress in Materials Science.* **55**(4), 247 (2010).

For Peer Review

68. J.A. Muñoz, M.S. Lucas, O. Delaire, M.L. Winterrose, L. Mauger, C.W. Li, A.O. Sheets, M.B. Stone, D.L. Abernathy, Y. Xiao, P. Chow and B. Fultz: Positive Vibrational Entropy of Chemical Ordering in FeV *Physical Review Letters.* **107**(11), 115501 (2011).

For Peer Review

Figure Caption

FIG. 1. Calculate empirical parameters for those predicted single-phase HEA compositions:[14, 30, 39] (a) ΔH_{mix}^{liq} vs δ, (b) η–parameter vs ϕ–parameter, (c) Ω–parameter vs Δχ, (d) $\Delta H_{IM}/\Delta H_{mix}^{liq}$ vs κ_1^{cr}, (e) $\overline{VEC}$ vs ΔS_{ideal}^{conf}, and (f) $\overline{B}$ vs $\overline{G}$. The marked threshold values are obtained from the work by Gao et al.[48]

FIG. 2 Calculated equilibrium phase mole fraction as a function of temperature for (a) CrMoNbTaTiVW, (b) CrMoNbReTaTiVW, and (c) CrFeMoNbReRuTaVW, using the TCNI8 database.[51] The insets are the corresponding Scheil simulations.

FIG. 3. Calculated total entropy of mixing at T=1273 K using the TCNI8 database[51] for: (a) the FCC phase in the Co-Cr-Fe-Ni system; (b) the FCC phase in the $CoCr_x$, $CoFeCr_x$, $CoFeNiCr_x$, and $CoFeMnNiCr_x$ systems; (c) the BCC phase in the Mo-Nb-Ta-W system, and (d) the BCC phase in the MoV_x, $MoNbV_x$, $MoNbTaV_x$, and $MoNbTaWV_x$ systems. The star symbols in (b) and (d) mark the equimolar compositions. The dashed curves represent ideal mixing.

FIG. 4. (a) Enthalpy of formation (ΔH_{ss}) vs SQS configurations for FCC CoCrFeNi, BCC MoNbTaW and HCP CoOsReRu. (b) DFT-calculated enthalpy of formation vs atomic size difference for various single-phase HEAs with the FCC (blue), BCC (green) and HCP (red) structures at zero temperature.

FIG. 5. DFT-calculated electronic DOS for (a) FCC CoCrFeNi, (b) BCC MoNbTaW and (c) HCP CoOsReRu. The vertical dashed lines mark the Fermi level.

FIG. 6. (a) DFT-calculated vibrational DOS using the harmonic approximation. The experimental data for FCC CoCrFeNi was measured by Lucas et al.[54] (b) DFT-calculated

For Peer Review

vibrational heat capacity at constant volume. (c) DFT- and MC/MD-predicted entropies of mixing from lattice configurations (S^{conf}), phonon vibration (ΔS_{mix}^{vib}), and electron excitation (ΔS_{mix}^{elec}). (d) Total entropy of mixing based on (c).

FIG. 7. Comparison between DFT calculations and the ROM in: (a) lattice parameter (a), (b-d) single-crystal elastic constants (C_{11}, C_{12}, and C_{44}), (e) polycrystalline bulk modulus (B), (f) polycrystalline shear modulus (G), and (g) polycrystalline Poisson's ratio (ν). The data shown are taken from the work by Gao et al.,[36] Feng and Widom,[59] Tian et al., [60] and Ge et al.[61]

FIG. 8. Distribution in the change of calculated properties (a, C_{11}, C_{12}, C_{44}, B, G, and ν) with respect to the averaged properties. The alloy number is provided in Table S4 Supplementary Materials.

For Peer Review

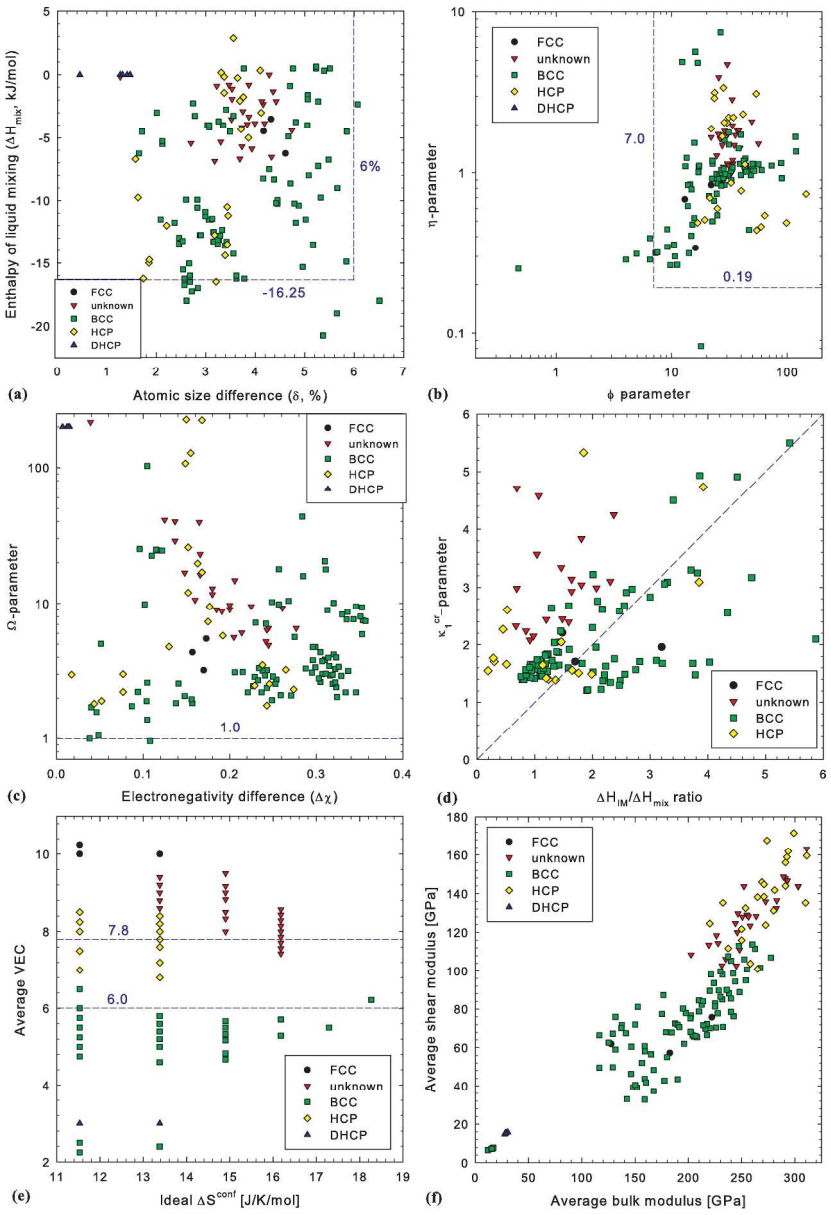

Figure 1.

220x320mm (300 x 300 DPI)

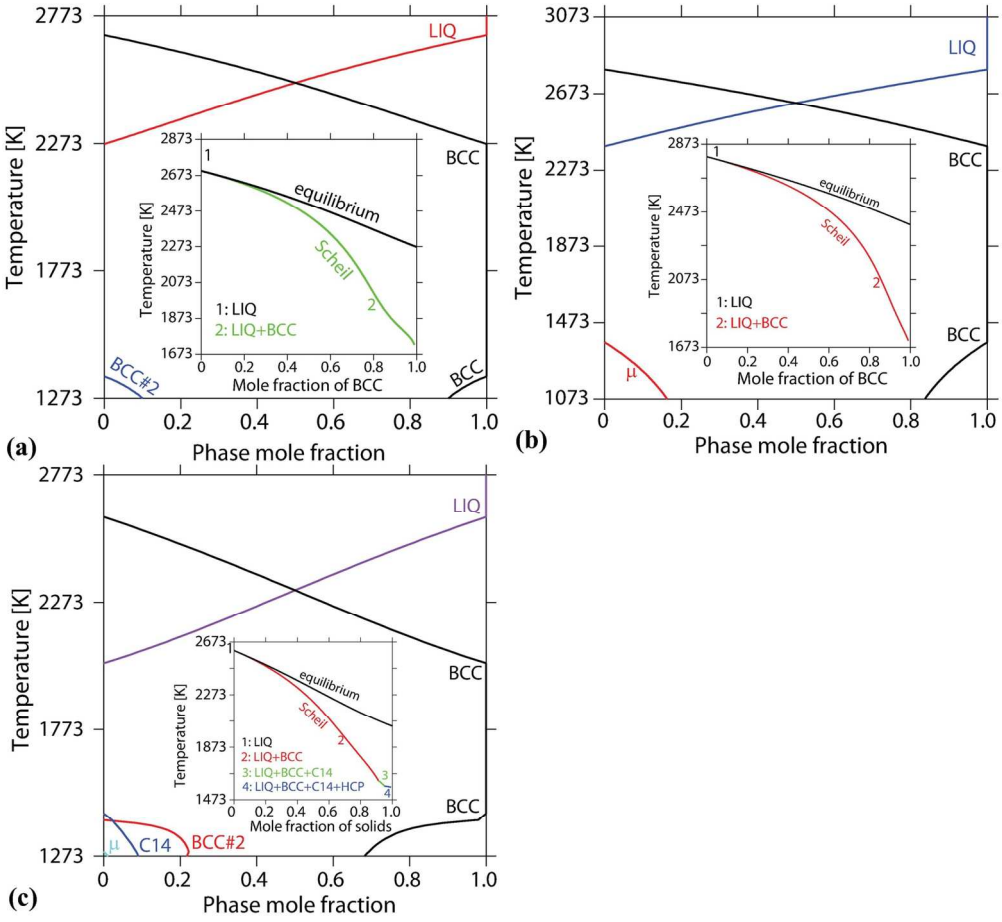

Figure 2

145x133mm (300 x 300 DPI)

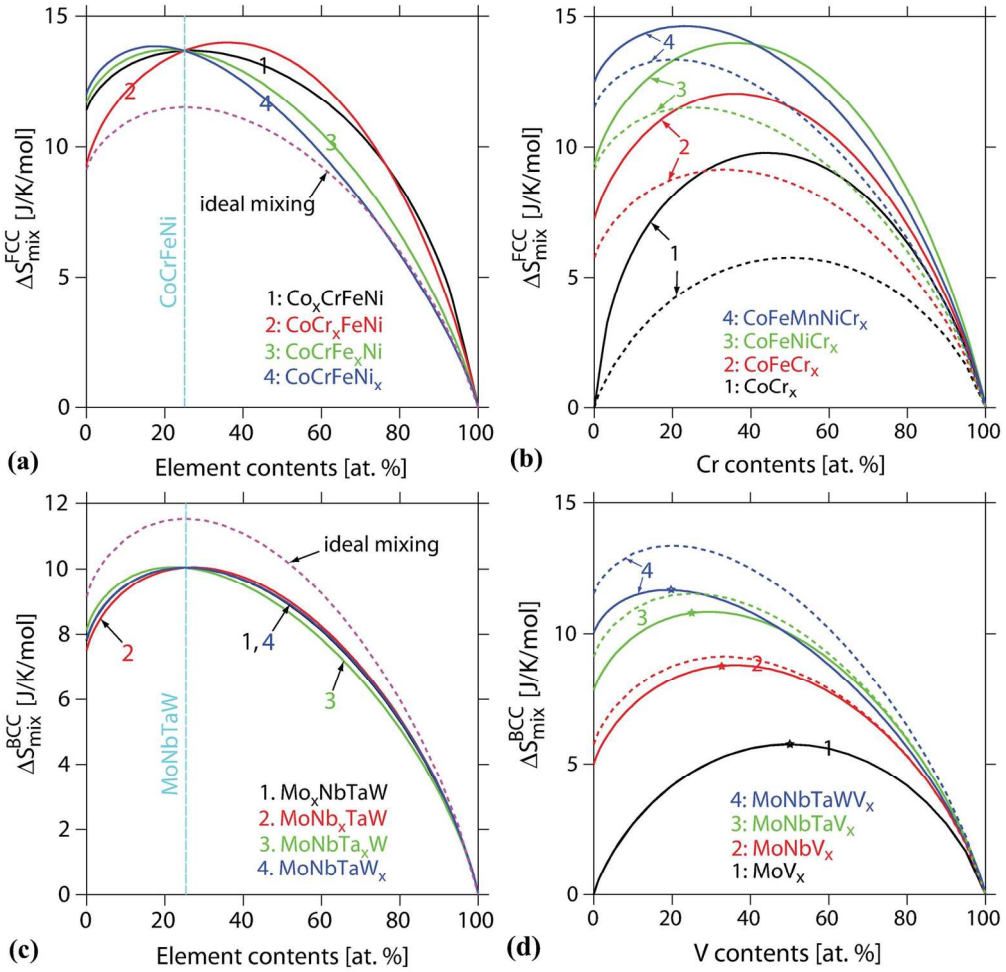

Figure 3

150x145mm (300 x 300 DPI)

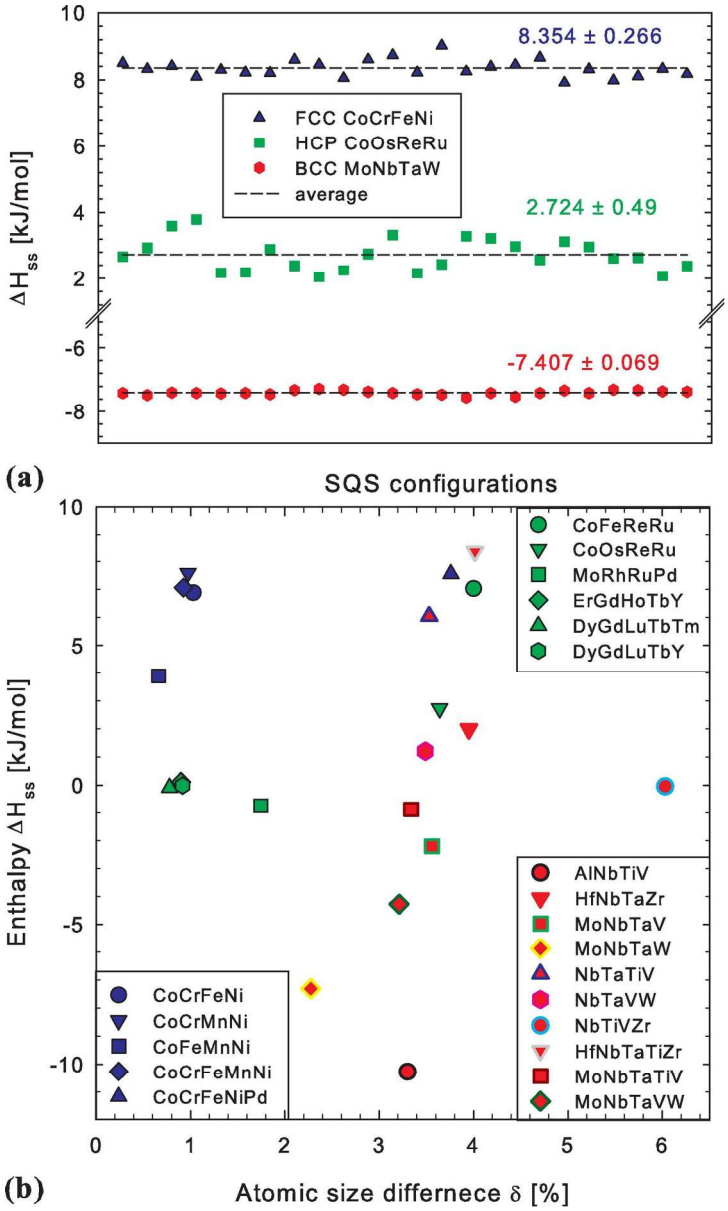

Figure 4

124x207mm (300 x 300 DPI)

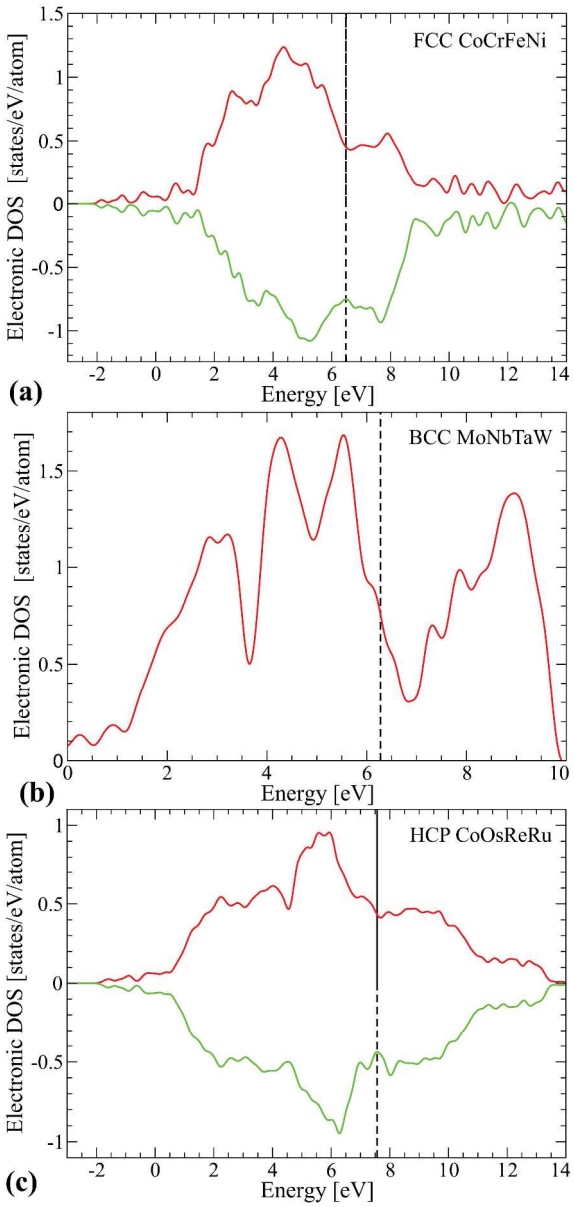

Figure 5

260x551mm (300 x 300 DPI)

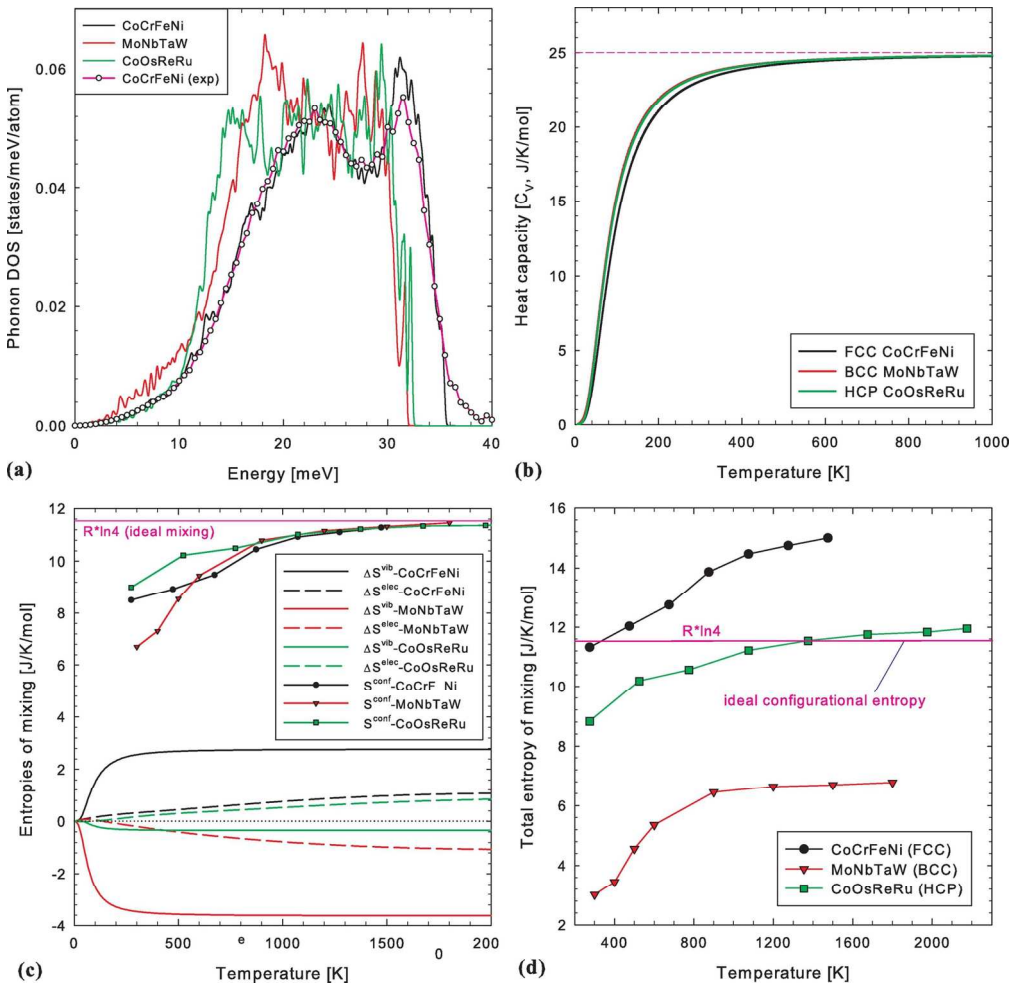

Figure 6

148x144mm (300 x 300 DPI)

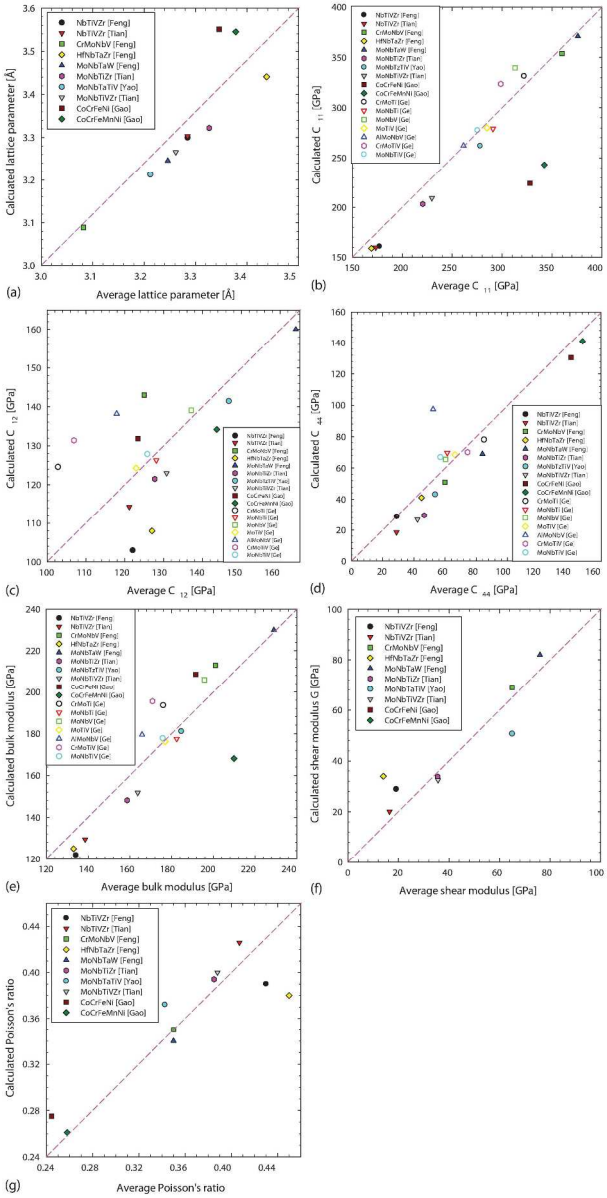

Figure 7

200x395mm (300 x 300 DPI)

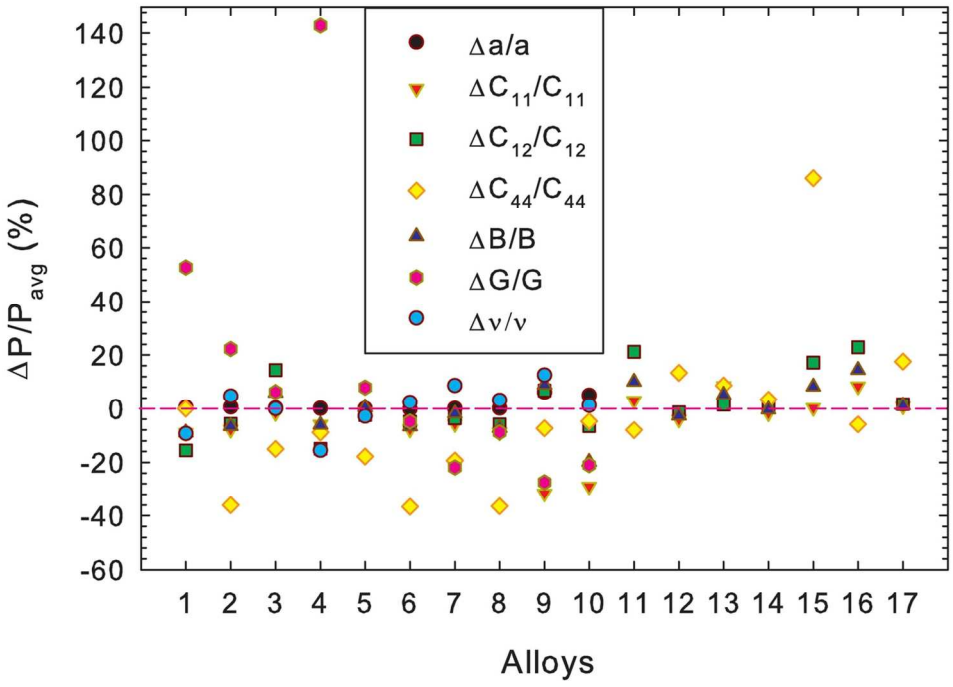

Figure 8

120x92mm (300 x 300 DPI)

eview

Supplementary Materials

Computational Modeling of High-Entropy Alloys: Structures, Thermodynamics and Elasticity

M. C. Gao[1,2*], P. Gao[3], J. A. Hawk[1], L.Z. Ouyang[3], D. E. Alman[1], and M. Widom[4]

[1]National Energy Technology Laboratory, Albany, OR 97321, USA.

[2]AECOM, P.O. Box 1959, Albany, OR 97321, USA.

[3]Tennessee State University, Nashville, TN 37209, USA.

[4]Carnegie Mellon University, Pittsburgh, PA 15213, USA.

*Correspondence: michael.gao@netl.doe.gov. Tel: +1-541-967-5869. Fax: +1-541-918-4493

For Peer Review

Empirical thermo-physical rules

The following equations are used to calculate those empirical thermos-physical parameters presented in the main text. These parameters are ideal configurational entropy (ΔS_{ideal}^{conf}), enthalpy of mixing of the liquid phase (ΔH_{mix}^{liq}),[1] atomic size difference (δ),[1] melting point of the alloy (T_m),[2] Ω-parameter,[2] valence electron concentration ($\overline{VEC}$),[3] the electronegativity difference ($\Delta\chi$),[4] the ϕ-parameter,[5] the η–parameter through the enthalpy of formation of the most stable binary compound ($|\Delta H_{ij}^{IM}|^{\max}$),[6] the average density ($\overline{\rho_m}$), the average bulk modulus ($\overline{B_m}$), and average shear modulus ($\overline{G_m}$):

$$\Delta S_{ideal}^{conf} = -R\sum_{i=1}^{N} c_i \ln c_i \tag{S1}$$

$$\Delta H_{mix}^{liq} = 4\sum_{i=1, i\neq j}^{N} \Delta H_{ij}^{liq} c_i c_j \tag{S2}$$

$$\delta = 100\,\%\sqrt{\sum_{i=1}^{N} c_i\left(1 - r_i / \sum_{j=1}^{N} c_j r_j\right)^2} \tag{S3}$$

$$\overline{T_m} = \sum_i c_i T_m^i \tag{S4}$$

$$\Omega = \frac{\overline{T_m}\Delta S_{ideal}^{conf}}{\left|\Delta H_{mix}^{liq}\right|} \tag{S5}$$

$$\overline{VEC} = \sum_i c_i VEC^i \tag{S6}$$

$$\Delta\chi = \sqrt{\sum_{i=1}^{N} c_i \left(\chi_i - \sum_{j=1}^{N} c_j \chi_j\right)^2} \tag{S7}$$

$$\phi = \frac{k_B \Delta S_{ideal}^{conf} - |\Delta H_{mix}^{liq}| / \overline{T_m}}{|S_E|} \tag{S8}$$

$$\eta = \frac{T_{ann}\Delta S_{ideal}^{conf}}{|\Delta H_{ij}^{IM}|^{\max}} \tag{S9}$$

$$\overline{\rho_m} = \frac{\sum_{i=1}^{N} c_i W_i}{\sum_{i=1}^{N} c_i W_i / \rho_i} \tag{S10}$$

$$\overline{B_m} = \sum_{i=1}^{N} c_i B_i \tag{S10}$$

$$\overline{G_m} = \sum_{i=1}^{N} c_i G_i \tag{S11}$$

where the individual items involved are defined as:

- c_i (and c_j) are the atomic percentage of the i^{th} (and j^{th}) element.
- r_i (and r_j) are the atomic radius of the i^{th} (and j^{th}) element.
- χ_i (and χ_j) are the Pauling electronegativity of the i^{th} (and j^{th}) element.
- T_m^i is the melting point of the i^{th} element.
- R is the gas constant (8.314 $J \cdot K^{-1} \cdot mol^{-1}$); k_B is the Boltzmann constant.
- S_E is the excessive entropy of mixing that is modeled as a function of atomic packing and atom size, and can be calculated following the procedure detailed in Ref.[5]

For Peer Review

- ΔH_{ij}^{liq} is the enthalpy of mixing of equimolar *i-j* binary liquid alloy, which is taken from Ref.[7-9]
- H_{ij}^{IM} stands for the enthalpy of formation of the most stable compound of the *i-j* binary system, and can be found from Ref.[10]
- W_i, B_i, G_i, and ρ_i are the atomic weight, bulk modulus, shear modulus and density of the i^{th} element, respectively.

For Peer Review

Table S1. Calculated empirical parameters for various equimolar single-phase alloys that were predicted using CALPHAD and phase diagram inspection with the FCC, BCC, and HCP structures.

Alloy	$\overline{\rho_m}$	$\overline{B_m}$	$\overline{G_m}$	ΔH_{mix}^{liq}	ΔS_{ideal}^{conf}	$\overline{T_m}$	Ω	δ [%]	ε [%]	Δχ	$\overline{VEC}$	ϕ	η
FCC structure													
CuMnNiZn	8.03	128	62	-3.5	11.53	1324	4.36	4.32	4.3	0.157	10	16.05	0.34
CuNiPdPt	13.32	183	57	-6.25	11.53	1739	3.21	4.61	4.62	0.17	10.2	12.96	0.684
CuNiPdPtRh	13.14	222	76	-4.48	13.38	1838	5.49	4.17	4.19	0.173	10	21.9	0.84
CoFeIrOsRh	15.44	291	148	-3.52	13.38	2372	9.02	3.52	3.53	0.185	8.6	33.46	2.87
CoIrNiOsRh	15.71	293	147	-0.8	13.38	2356	39.4	3.87	3.88	0.165	9	30.36	4.73
CoIrNiPdRh	13.38	248	111	0	13.38	2060	200	4.28	4.29	0.165	9.4	25.5	3.93
CoIrOsPtRh	18.02	303	144	-1.92	13.38	2418	16.85	3.53	3.56	0.148	9	35.64	1.72
Unknown[*a]													
IrNiOsPtRh	18.03	303	144	-1.12	13.38	2410	28.8	3.53	3.56	0.137	9.2	36.57	1.86
IrOsPtRhRu	18.35	311	163	-0.16	13.38	2586	216.29	1.27	1.26	0.0392	8.8	282.87	3.65
NiOsPtRhRu	15.93	283	136	-0.8	13.38	2384	39.88	3.47	3.49	0.137	9	38.2	1.84
CoCrFeMnNiOs	10.86	203	108	-5.44	14.9	2052	5.61	2.7	2.69	0.205	8	56.48	1.52
CoCrFeNiOsRh	11.72	246	120	-5.33	14.9	2172	6.07	3.3	3.29	0.214	8.33	39.04	1.43
CoCrFeNiOsRe	13.42	244	125	-3.33	14.9	2375	10.62	3.87	3.86	0.16	8	30.58	1.74
CoFeIrNiOsRh	14.49	273	136	-2.89	14.9	2265	11.68	3.75	3.75	0.18	8.83	33.5	1.98
CoFeIrNiPdRh	12.53	235	106	-2.33	14.9	2019	12.89	4.16	4.16	0.18	9.17	27.44	1.48
CoIrNiOsPtRh	16.76	283	132	-2.11	14.9	2303	16.25	4.13	4.15	0.166	9.17	28.7	1.83
CoIrNiPdPtRh	14.86	245	103	-1.33	14.9	2057	22.98	4.36	4.39	0.166	9.5	26.26	1.63
IrNiOsPtRhRu	17.09	289	149	-0.89	14.9	2443	40.95	3.22	3.25	0.125	9	49.34	2.1
CoCrFeMnNiOsRh	11.11	228	114	-6.86	16.18	2078	4.9	3.18	3.17	0.245	8.14	43.2	1.02

For Peer Review

CoCrFeMnOsReRh	13.01	255	129	-5.71	16.18	2326	6.58	3.73	3.73	0.245	7.71	33.86	1.14
CoCrFeMnNiOsRe	12.58	226	118	-4.16	16.18	2253	8.76	3.73	3.72	0.191	7.86	34.75	1.49
CoCrFeNiOsReRh	13.27	264	128	-3.92	16.18	2356	9.73	3.84	3.84	0.2	8.14	33.73	1.2
CoCrFeNiPdReRh	11.59	231	103	-3.84	16.18	2144	9.04	4.19	4.19	0.2	8.43	28.07	1.09
CoCrMnNiOsReRh	13.19	256	128	-5.88	16.18	2314	6.37	3.93	3.93	0.243	8	30.29	1.14
CoCrMnNiOsReW	14.36	246	130	-4.41	16.18	2522	9.26	4.74	4.74	0.261	7.57	21.94	1.67
CoFeMnNiOsReRh	13.3	258	123	-3.84	16.18	2261	9.54	3.99	3.99	0.225	8.29	31.14	1.11
CoFeIrMnNiOsRh	13.51	251	128	-6.69	16.18	2158	5.22	3.69	3.69	0.242	8.57	32.93	1
CrMnNiOsReRuW	14.71	252	144	-6.53	16.18	2642	6.55	4.33	4.33	0.277	7.43	25.29	1.75
CoFeMnOsReZn	12.88	219	113	-2.11	14.9	2093	14.77	4.42	4.43	0.206	8.5	24.51	1.28
BCC structure													
AlCrFeMn	5.98	132	76	-9.75	11.53	1611	1.9	5.32	5.28	0.104	6	6.49	0.287
AlCrFeMo	6.85	159	61	-7.25	11.53	1955	3.11	5.27	5.28	0.215	5.75	9.74	0.265
AlCrFeV	5.68	142	68	-11.75	11.53	1777	1.74	4.82	4.81	0.087	5.5	7.23	0.316
AlCrMnMo	6.77	147	60	-6.75	11.53	1882	3.21	5.48	5.5	0.243	5.5	9.16	0.445
AlCrMnTi	5.16	117	66	-18	11.53	1643	1.05	6.51	6.54	0.0485	5	0.47	0.252
AlCrMnV	5.61	129	67	-11.5	11.53	1704	1.71	5.02	5.01	0.0402	5.25	6.49	0.391
AlCrMoV	6.46	157	52	-8.25	11.53	2048	2.86	4.16	4.18	0.229	5	15.12	0.477
AlCrVW	8.92	177	87	-7.5	11.53	2248	3.45	4.28	4.3	0.315	5	15.66	0.524
AlFeMnV	5.76	132	59	-13.5	11.53	1612	1.38	5.17	5.17	0.105	5.75	4.02	0.287
AlFeMoV	6.61	159	44	-10.25	11.53	1956	2.2	4.45	4.47	0.221	5.5	11.14	0.266
AlFeTiV	5.04	129	50	-20.75	11.53	1717	0.954	5.37	5.4	0.108	5	-0.68	0.264
AlMnTiV	4.98	117	49	-19	11.53	1644	0.997	5.65	5.69	0.0383	4.75	-0.04	0.252
AlMoNbV	6.93	159	33	-11.5	11.53	2191	2.2	3.1	3.11	0.237	4.75	22.54	0.5
AlNbVW	9.16	179	68	-11.5	11.53	2390	2.4	3.06	3.07	0.323	4.75	24.85	0.545

For Peer Review

BaCaEuSr	3.28	12	7	0.5	11.53	1066	24.57	4.76	4.77	0.116	2.25	16.81	4.84
BaCaEuYb	4.22	16	8	0.5	11.53	1078	24.84	5.51	5.48	0.115	2.5	12.31	4.9
BaEuSrYb	4.35	15	7	0.5	11.53	1062	24.47	5.23	5.25	0.122	2.5	13.99	59.61
BaCaEuYb	4.22	16	8	0.5	11.53	1078	24.84	5.51	5.48	0.115	2.5	12.31	4.9
CaEuSrYb	4	17	8	0.5	11.53	1090	25.13	3.77	3.76	0.096	2.5	26.54	7.46
CrFeMnV	7.11	153	81	-2.25	11.53	1923	9.85	2.74	2.73	0.102	6.5	46.68	0.442
CrFeTiV	6.2	150	72	-9	11.53	2029	2.6	5.66	5.65	0.105	5.75	7.52	0.319
CrMnTiV	6.12	138	72	-4.5	11.53	1956	5.01	5.85	5.84	0.0512	5.5	9.18	0.345
CrMoNbV	8.15	180	55	-4	11.53	2502	7.21	5.05	5.07	0.23	5.5	13.48	1.24
CrMoTiV	6.94	165	57	-3.75	11.53	2300	7.07	4.82	4.83	0.242	5.25	14.81	0.406
FeMoTiV	7.08	168	48	-8	11.53	2208	3.18	5.08	5.11	0.238	5.75	10.66	0.3
MoNbReTa	13.93	243	76	-17	11.53	3099	2.1	2.84	2.84	0.259	5.75	25.81	0.901
MoNbReTi	10.67	220	70	-16.5	11.53	2762	1.93	2.68	2.69	0.249	5.5	26.54	0.898
MoNbReV	11.4	233	71	-13.25	11.53	2822	2.45	3.15	3.15	0.227	5.75	23.39	0.918
MoNbTaTi	10.03	178	43	-3	11.53	2719	10.45	2.01	2.02	0.268	5	89.82	0.926
MoNbTaV	10.68	190	44	-3.25	11.53	2780	9.86	3.56	3.58	0.257	5.25	28.35	0.946
MoNbTiV	7.35	168	37	-2.75	11.53	2443	10.24	3.41	3.43	0.249	5	30.99	0.961
MoNbTiW	10.42	205	66	-5.5	11.53	2821	5.91	2.12	2.12	0.353	5.25	73.3	1.11
MoNbVW	11.13	218	67	-4	11.53	2881	8.3	3.03	3.03	0.33	5.5	37.92	1.42
MoReTaTi	12.88	228	78	-16	11.53	2897	2.09	2.68	2.69	0.271	5.5	28.7	0.842
MoReTaV	13.75	240	79	-12.5	11.53	2957	2.73	3.15	3.15	0.254	5.75	24.99	0.86
MoReTaW	16.76	278	107	-11.75	11.53	3335	3.27	2.37	2.36	0.322	6	48.45	0.97
MoReTiV	10.25	218	72	-12.75	11.53	2620	2.37	2.88	2.88	0.243	5.5	27.42	0.911
MoReTiW	13.39	255	101	-11.5	11.53	2998	3	2.09	2.08	0.307	5.75	60.2	1.04
MoReVW	14.33	268	102	-6.25	11.53	3058	5.64	1.65	1.66	0.275	6	119.65	1.36

For Peer Review

MoTiVW	10	203	68	-3.25	11.53	2679	9.5	2.78	2.78	0.346	5.25	45.96	1.05
NbReTaTi	12.33	213	82	-18	11.53	2860	1.83	2.61	2.63	0.157	5.25	26.85	0.831
NbReTaV	13.13	225	83	-16.25	11.53	2921	2.07	3.78	3.79	0.148	5.5	14.45	0.849
NbReTaW	16.05	263	112	-17.25	11.53	3299	2.2	2.72	2.73	0.334	5.75	29.38	0.959
NbReTiV	9.78	203	77	-16.25	11.53	2583	1.83	3.62	3.63	0.138	5.25	13.81	0.84
NbReTiW	12.81	240	105	-16.75	11.53	2961	2.04	2.57	2.57	0.324	5.5	30.69	0.963
NbReVW	13.67	253	106	-13.25	11.53	3022	2.63	3.16	3.16	0.305	5.75	24.38	0.983
NbTaTiW	12.07	198	78	-4.5	11.53	2919	7.48	1.71	1.72	0.354	5	118.29	1.68
NbTaVW	12.85	210	79	-4.5	11.53	2980	7.63	3.49	3.51	0.343	5.25	28.63	1.6
NbTiVW	9.54	188	73	-4	11.53	2642	7.61	3.35	3.36	0.335	5	31.1	1.79
ReTaTiV	12.05	210	85	-16	11.53	2718	1.96	3.62	3.63	0.156	5.25	14.87	0.79
ReTaTiW	15.01	248	113	-16.25	11.53	3096	2.2	2.57	2.57	0.346	5.5	32.83	0.9
ReTaVW	16	260	114	-12.5	11.53	3157	2.91	3.16	3.16	0.329	5.75	25.83	0.918
ReTiVW	12.55	238	108	-12.75	11.53	2820	2.55	2.9	2.9	0.319	5.5	28.49	0.98
TaTiVW	11.77	195	80	-4	11.53	2777	8	3.35	3.36	0.351	5	31.33	1.5
BaCaEuSrYb	3.87	15	7	0.64	13.38	1072	22.42	5.23	5.23	0.11	2.4	16.01	5.66
AlCrFeMnV	6.01	137	70	-10.4	13.38	1725	2.22	4.88	4.86	0.0941	5.8	10.45	0.357
AlCrFeMoV	6.7	159	58	-8.64	13.38	2001	3.1	4.71	4.72	0.206	5.6	14.11	0.315
AlCrMnTiV	5.34	125	63	-14.88	13.38	1751	1.57	5.84	5.85	0.0462	5	4.97	0.312
AlCrNbVW	8.84	175	77	-10.24	13.38	2348	3.07	4.79	4.82	0.295	5	13.81	0.622
HfMoNbTiZr	8.7	142	33	-1.6	13.38	2444	20.44	5.06	5.07	0.31	4.6	17.17	1.09
HfMoTaTiZr	10.21	148	39	-1.92	13.38	2552	17.79	5.06	5.07	0.311	4.6	17.04	1.01
MoNbTaTiW	11.75	204	66	-5.28	13.38	2914	7.39	2.12	2.13	0.357	5.2	88.83	1.15
MoNbReTiW	12.33	238	88	-13.44	13.38	2948	2.94	2.46	2.46	0.316	5.6	50.14	1.11
MoNbTiVW	9.69	196	62	-4.16	13.38	2693	8.66	3.07	3.08	0.336	5.2	43.45	1.23

For Peer Review

MoNbReTaTi	11.95	216	70	-15.04	13.38	2867	2.55	2.66	2.67	0.253	5.4	39.73	0.968
MoNbReTaV	12.58	226	70	-13.28	13.38	2916	2.94	3.42	3.43	0.241	5.6	25.91	0.984
MoNbReTiV	9.87	208	65	-13.12	13.38	2646	2.7	3.27	3.28	0.233	5.4	27.06	0.999
MoNbReVW	13	248	89	-10.56	13.38	2997	3.8	2.83	2.83	0.296	5.8	41.96	1.13
MoReTaTiV	11.7	214	72	-12.8	13.38	2754	2.88	3.27	3.28	0.25	5.4	28.06	0.929
MoReTaTiW	14.11	244	94	-12.96	13.38	3056	3.16	2.46	2.46	0.337	5.6	51.95	1.03
MoReTaVW	14.87	254	95	-9.92	13.38	3105	4.19	2.83	2.83	0.32	5.8	43.36	1.05
MoReTiVW	12.09	236	90	-9.92	13.38	2835	3.82	2.6	2.59	0.31	5.6	50.22	1.14
MoTaTiVW	11.49	202	68	-4	13.38	2801	9.37	3.07	3.08	0.353	5.2	43.88	1.11
NbReTaTiW	13.63	232	98	-15.52	13.38	3027	2.61	2.54	2.55	0.322	5.4	44.35	1.02
NbReTaVW	14.34	242	99	-13.6	13.38	3075	3.03	3.39	3.4	0.311	5.6	26.9	1.04
NbReTaTiV	11.28	202	75	-14.24	13.38	2725	2.56	3.56	3.58	0.141	5.2	22.37	0.92
NbReTiVW	11.65	224	94	-13.44	13.38	2806	2.79	3.24	3.25	0.303	5.4	28.17	1.06
NbTaTiVW	11.08	190	72	-3.68	13.38	2772	10.08	3.26	3.28	0.32	5	39.81	1.73
NbTaTiVZr	8.48	146	46	0.32	13.38	2458	102.8	5.39	5.41	0.105	4.6	15.73	1.54
ReTaTiVW	13.47	230	100	-13.12	13.38	2914	2.97	3.24	3.25	0.319	5.4	29.11	0.983
AlCrMoNbVW	9.08	184	68	-8.33	14.9	2440	4.36	4.38	4.41	0.305	5.17	21.06	0.719
HfMoNbTaTiZr	9.95	152	39	-0.889	14.9	2585	43.33	4.7	4.7	0.284	4.67	22.56	1.14
HfMoTaTiVZr	9.69	150	41	-2.33	14.9	2491	15.9	6.07	6.09	0.285	4.67	13.15	1.1
MoNbReTaTiV	11.13	207	66	-12.33	14.9	2753	3.33	3.33	3.34	0.234	5.33	32.47	1.03
MoNbReTaTiW	13.11	232	85	-13.22	14.9	3005	3.39	2.53	2.54	0.326	5.5	56.48	1.13
MoNbReTaVW	13.68	240	86	-11.44	14.9	3046	3.96	3.13	3.13	0.314	5.67	39.1	1.14
MoNbReTiVW	11.43	225	81	-11.22	14.9	2821	3.74	2.99	2.99	0.307	5.5	42.02	1.19
MoNbTaTiVZr	8.75	160	42	-2.11	14.9	2531	17.86	5.27	5.27	0.257	4.83	17.27	1.11
MoReTaTiVW	12.95	230	87	-10.89	14.9	2911	3.98	2.99	2.99	0.323	5.5	42.93	1.09

For Peer Review

NbReTaTiVW	12.57	220	90	-12.78	14.9	2886	3.37	3.29	3.3	0.299	5.33	33.64	1.08
CrMoNbTaTiVW	10.54	191	71	-4.9	16.18	2705	8.94	4.67	4.71	0.313	5.29	23.28	0.671
CrMoNbReTaVW	12.95	229	90	-9.96	16.18	2922	4.75	4.45	4.48	0.299	5.71	22.53	1.19
CrMoNbReTaTiVW	11.77	214	84	-10.19	17.29	2799	4.75	4.42	4.45	0.296	5.5	24.56	0.742
CrFeMoNbReRuTaVW	12.44	221	98	-15.31	18.27	2763	3.3	4.96	4.98	0.288	6.22	17.97	0.083
HCP structure													
CoCrReRu	12.87	233	135	-5	11.53	2504	5.77	3.86	3.87	0.192	7.5	22.01	1.89
CoOsReRu	16.73	294	162	-0.25	11.53	2785	128.4	3.64	3.67	0.155	8	30.24	2.06
CoPtReRu	16.45	250	122	-3	11.53	2469	9.49	4.12	4.15	0.177	8.5	21.39	0.699
CrIrMoRh	13.28	273	124	-16.5	11.53	2513	1.76	3.21	3.22	0.243	7.5	16.77	0.489
CrIrRhW	15.81	293	159	-13.5	11.53	2713	2.32	3.43	3.45	0.274	7.5	19.27	0.509
CrMoOsRu	13.23	254	133	-12.75	11.53	2747	2.48	3.18	3.18	0.229	7	23.59	3.17
CrOsRuW	15.77	274	168	-10.5	11.53	2947	3.24	3.43	3.43	0.265	7	23.37	2.93
CoPtReRu	16.45	250	122	-3	11.53	2469	9.49	4.12	4.15	0.177	8.5	21.39	0.699
IrMoPdRu	14.23	238	112	-9.75	11.53	2518	2.98	1.63	1.63	0.0173	8.25	98.72	0.489
IrMoRhW	16.13	310	135	-15	11.53	2892	2.22	1.85	1.85	0.0768	7.5	63.83	0.543
IrMoPtRu	16.58	250	116	-16.25	11.53	2571	1.82	1.74	1.74	0.0436	8.25	59.36	0.462
MoOsRuW	16.1	291	144	-12	11.53	3126	3	2.21	2.21	0.0768	7	54.03	3.11
MoPtRhRu	14.14	265	101	-14.75	11.53	2445	1.91	1.86	1.86	0.052	8.25	54.53	0.439
CoCrFeReRu	11.94	220	125	-4.32	13.38	2365	7.33	3.71	3.71	0.175	7.6	28.61	2.07
CoFeOsReRu	15.13	269	146	-1.76	13.38	2590	19.69	3.76	3.77	0.163	8	31.17	2.22
CoIrOsReRu	17.97	299	172	-1.44	13.38	2776	25.79	3.37	3.4	0.152	8.2	40.05	0.773
CoNiOsReRu	15.4	271	145	0.32	13.38	2574	107.62	4.1	4.12	0.149	8.4	27.37	1.69
CoOsPdReRu	15.71	271	138	2.88	13.38	2594	12.05	3.56	3.59	0.152	8.4	34.13	2.22
CoOsPtReRu	17.71	281	142	-2.08	13.38	2636	16.96	3.69	3.72	0.168	8.4	32.58	0.867

For Peer Review

CoOsReRhRu	15.85	311	160	0.16	13.38	2675	223.76	3.31	3.33	0.168	8.2	43	1.13
CoOsReRuTc	15.63	291	156	-0.16	13.38	2714	226.99	3.37	3.4	0.15	7.8	41.48	2.33
CrIrMoRhW	14.61	280	131	-14.4	13.38	2749	2.55	3.39	3.4	0.246	7.2	24.83	0.599
CrMoOsRuW	14.58	265	138	-11.2	13.38	2937	3.51	3.45	3.46	0.238	6.8	28	3.39
MoPdRhRuTc	11.69	258	104	-6.72	13.38	2400	4.78	1.58	1.58	0.13	8	145.65	0.738
210 quaternary RE HEAs[*b]													
378 quinary RE HEAs[*b]													
210 senary RE HEAs[*b]													
120 septenary RE HEAs[*b]													
45 octonary RE HEAs[*b]													
10 Ennead RE HEAs[*b]													
1 decadal RE HEA[*b]													
DHCP structure													
CeNdPmPr	6.93	29	16	0	11.53	1237	200**	0.455	0.455	0.0071	3	1914.43	inf
CeLaPmPr	6.7	28	15	0	11.53	1211	200**	1.41	1.41	0.0122	3	198.59	inf
CeLaNdPr	6.64	28	15	0	11.53	1192	200**	1.27	1.27	0.015	3	241.79	inf
CeLaNdPm	6.76	29	16	0	11.53	1233	200**	1.47	1.46	0.015	3	182.45	inf
LaNdPmPr	6.78	30	16	0	11.53	1268	200**	1.47	1.46	0.015	3	182.45	inf
CeLaNdPmPr	6.76	29	15	0	13.38	1228	200**	1.32	1.31	0.014	3	262.39	inf

[*a] The crystal structures of these compositions were not suggested in Ref.[10] although the majority of them likely prefer an FCC structure.

*[b] These numbers represent the total number of equimolar compositions for quaternary, quinary, senary, septenary, octonary, ennead and decadal systems respectively, which comprises arbitrary selection of RE elements from the Dy-Er-Gd-Ho-Lu-Sc-Sm-Tb-Tm-Y system.[11]

**Since the enthalpy of mixing is zero for these alloys, the Ω–parameter will be infinity. In order to show these compositions in Figure 1(b), the Ω-parameter is set as 200 arbitrarily to demonstrate that they have an extremely large Ω-parameter.

For Peer Review

Table S2. DFT-calculated lattice parameter [a, Å], single-crystal elastic constants, polycrystalline bulk modulus, polycrystalline shear modulus, and polycrystalline Poisson's ratio for those pure elements that constitute BCC HEAs in the present work as presented in Figure 6, taken from the work by Feng and Widom.[12]

BCC	*Cr.cI2*	*Hf.cI2*	*Mo.cI2*	*Nb.cI2*	*Ta.cI2*	*Ti.cI2*	*V.cI2*	*Zr.cI2*	*W.cI2*
a	2.857	3.541	3.159	3.322	3.319	3.254	2.99	3.571	3.184
C_{11}	444	73	469	247	268	95	278	87	519
C_{12}	62	116	159	137	161	115	143	93	199
C_{44}	99	53	101	17	79	41	24	34	141
B	188	102	263	173	197	108	188	91	306
G	129	-54	120	28	67	-10	37	5	149
ν	0.22	0.83	0.3	0.42	0.35	0.55	0.41	0.47	0.29

For Peer Review

Table S3. DFT-calculated lattice parameter [a, Å], single-crystal elastic constants [GPa], polycrystalline bulk modulus [GPa], polycrystalline shear modulus [GPa], and polycrystalline Poisson's ratio for those pure elements that constitute FCC HEAs in the present work as presented in Figure 6, taken from the work by Gao et al.[13] and the present work. "FM" stands for ferromagnetism, and "AFM" stands for antiferromagnetism.

FCC	*Co.hP2_FM*	*Co.cF4*	*Cr.cF4*	*Cr.cI2_AFM*	*Fe.cF4_FM*	*Fe.cF4_AFM*	*Mn.cF4*	*Ni.cF4*
a	3.523	3.523	3.625	2.870	3.482	*a*=3.680 *b*=*c*=3.429	3.508	3.508
C_{11}	361	288	26	434	311	263	400	278
C_{12}	169	168	348	59	107	101	225	159
C_{44}	97	142	-87	96	192	267	178	133
C_{13}	114					101		
C_{33}	406					334		
C_{66}	96					177		
B	208	208	240	184	175	196	283	199
G	101	101	-112	126	149	132	134	96
ν	0.292	0.292	0.775	0.22	0.168	0.225	0.296	0.291

For Peer Review

Table S4. DFT-calculated lattice parameter [a, Å], single-crystal elastic constants [GPa], polycrystalline bulk modulus [GPa], polycrystalline shear modulus [GPa], polycrystalline Poisson's ratio, and in comparison with their average values estimated using the ROM. The data are collected from the work by Gao et al.,[13] Feng and Widom,[12] Tian et al., [14] and Ge et al.[15]

No.	Alloys	$\overline{a}$	a	$\overline{C_{11}}$	C_{11}	$\overline{C_{12}}$	C_{12}	$\overline{C_{44}}$	C_{44}	$\overline{B}$	B	$\overline{G}$	G	$\overline{\nu}$	ν
1	NbTiVZr[12]	3.284	3.300	177	161	122	103	29	29	134	122	19	29	0.43	0.39
2	NbTiVZr[14]	3.285	3.303	173	160	121	114	29	19	139	130	16	20	0.41	0.43
3	CrMoNbV[12]	3.082	3.089	360	354	125	143	60	51	201	213	65	69	0.35	0.35
4	HfNbTaZr[12]	3.438	3.441	169	159	127	108	45	41	133	125	14	34	0.45	0.38
5	MoNbTaW[12]	3.246	3.246	376	371	164	160	84	69	229	230	76	82	0.35	0.34
6	MoNbTiZr[14]	3.327	3.322	220	203	128	122	47	30	159	148	36	34	0.39	0.39
7	MoNbTaTiV[16]	3.212	3.213	278	262	147	141	54	43	185	181	65	51	0.34	0.37
8	MoNbTiVZr[14]	3.261	3.266	230	209	131	123	42	27	164	152	36	33	0.39	0.40
9	CoCrFeNi[13]	3.346	3.551	328	224	123	132	141	131	192	209	118	86	0.24	0.28
10	CoCrFeMnNi[13]	3.378	3.545	342	243	144	134	148	141	210	168	121	96	0.26	0.26
11	CrMoTi[15]			322	332	102.8	125	85	78.2	175.9	194		88		0.3
12	MoNbTi[15]			290.9	279	128.1	126	61.5	69.7	182.4	178		73		0.32
13	MoNbV[15]			313	340	137.1	139	60.4	65.6	195.7	206		78		0.33
14	MoTiV[15]			284.9	280	122.9	124	66.4	68.6	176.9	176		72		0.32
15	AlMoNbV[15]			261.4	262	117.9	138	52.4	97.5	165.8	180		81		0.3
16	CrMoTiV[15]			298.7	324	106.9	131	74.5	70.1	170.8	196		80		0.32
17	MoNbTiV[15]			275.3	278	125.8	128	57	67	175.7	178		70		0.33

For average property calculations, the properties of BCC Ti, BCC Cr, and ferromagnetic FCC Fe were used for the alloys cited in Ref. [12-14, 16] The data cited from Ref.[15] are taken as they are without alteration.

For Peer Review

References:

1. Y. Zhang, Y.J. Zhou, J.P. Lin, G.L. Chen and P.K. Liaw: Solid-Solution Phase Formation Rules for Multi-component Alloys *Adv. Eng. Mater.* **10**, 534 (2008).

2. Y. Zhang, Z.P. Lu, S.G. Ma, P.K. Liaw, Z. Tang, Y.Q. Cheng and M.C. Gao: Guidelines in predicting phase formation of high-entropy alloys *MRS Comm.* **4**, 57 (2014).

3. S. Guo, C. Ng, J. Lu and C.T. Liu: Effect of valence electron concentration on stability of fcc or bcc phase in high entropy alloys *J. Appl. Phys.* **109**, 103505 (2011).

4. S. Fang, X. Xiao, L. Xia, W. Li and Y. Dong: Relationship between the widths of supercooled liquid regions and bond parameters of Mg-based bulk metallic glasses *J. Non-Cryst. Solids.* **321**, 120 (2003).

5. Y.F. Ye, Q. Wang, J. Lu, C.T. Liu and Y. Yang: Design of high entropy alloys: A single-parameter thermodynamic rule *Scripta Mater.* **104**, 53 (2015).

6. O.N. Senkov and D.B. Miracle: A new thermodynamic parameter to predict formation of solid solution or intermetallic phases in high entropy alloys *J. Alloys Compd.* **658**, 603 (2016).

7. A. Takeuchi and A. Inoue: Classification of bulk metallic glasses by atomic size difference, heat of mixing and period of constituent elements and its application to characterization of the main alloying element *Mater. Trans.* **46**, 2817 (2005).

8. R.H. Taylor, F. Rose, C. Toher, O. Levy, K. Yang, M.B. Nardelli and S. Curtarolo: A RESTful API for exchanging materials data in the AFLOWLIB.org consortium *Comp. Mater. Sci.* **93**, 178 (2014).

9. Online sources: M. Widom: Alloy Database. Available at: http://alloy.phys.cmu.edu.

10. M.C. Troparevsky, J.R. Morris, P.R.C. Kent, A.R. Lupini and G.M. Stocks: Criteria for Predicting the Formation of Single-Phase High-Entropy Alloys *Phys. Rev. X.* **5**, 011041 (2015).

11. M.C. Gao, B. Zhang, S.M. Guo, J.W. Qiao and J.A. Hawk: High-Entropy Alloys in Hexagonal Close Packed Structure *Metall. Mater. Trans. A.* **47A**, 3322 (2016).

12. B. Feng and M. Widom: Elastic stability and lattice distortion of refractory high entropy alloys *Mater. Chem. Phys.* **in press**, (2017).

13. M.C. Gao, C. Niu, C. Jiang and D.L. Irving: Applications of Special Quasi-Random Structures to High-Entropy Alloys, in High-Entropy Alloys: Fundamentals and Applications, edited by M. C. Gao, J. W. Yeh, P. K. Liaw and Y. Zhang (Springer International Publishing, City, 2016), pp. 333.

14. L.Y. Tian, G. Wang, J.S. Harris, D.L. Irving, J. Zhao and L. Vitos: Alloying effect on the elastic properties of refractory high-entropy alloys *Mater. Des.* **114**, 243 (2017).

15. H.J. Ge, F.Y. Tian and Y. Wang: Elastic and thermal properties of refractory high-entropy alloys from first-principles calculations *Comp. Mater. Sci.* **128**, 185 (2017).

For Peer Review

16. H.W. Yao, J.W. Qiao, J.A. Hawk, H.F. Zhou, M.W. Chen and M.C. Gao: Mechanical properties of refractory high-entropy alloys: Experiments and modeling *J. Alloys Compd.* **696**, 1139 (2017).

For Peer Review